applied sciences

IMPACT FACTOR 2.9

CITESCORE 6.1

Review

System-Level Review and Advances in Axial-Flux Permanent-Magnet Machines: Topology Classification, Design Optimisation, Materials, Modelling, and Control Strategies

Roman Tangalychev, Maurizio Guadagno, Viktor Skrickij, Massimo Delogu and Valentin Ivanov

MDPI

https://doi.org/10.3390/app16146854

applied sciences

MDPI

Review

System-Level Review and Advances in Axial-Flux Permanent-Magnet Machines: Topology Classification, Design Optimisation, Materials, Modelling, and Control Strategies

Roman Tangalychev [1,*], Maurizio Guadagno [2], Viktor Skrickij [3], Massimo Delogu [2] and Valentin Ivanov [1]

[1] Smart Vehicle Systems Group, Control Engineering Group, Technische Universität Ilmenau, Robert-Bosch-Ring 1, 98693 Ilmenau, Germany; valentin.ivanov@tu-ilmenau.de
[2] Department of Industrial Engineering, University of Florence, Via di S. Marta 3, 50139 Florence, Italy; maurizio.guadagno@unifi.it (M.G.); massimo.delogu@unifi.it (M.D.)
[3] Faculty of Transport Engineering, Vilnius Gediminas Technical University, 10105 Vilnius, Lithuania; viktor.skrickij@vilniustech.lt
* Correspondence: roman.tangalychev@tu-ilmenau.de

Abstract

Axial-flux permanent-magnet (AFPM) machines are becoming an increasingly promising solution for electromechanical systems requiring high power density. In particular, their use is expanding to electric vehicles (EVs), the aerospace industry, and advanced industrial applications, such as renewable energy applications. Their compact design, high torque-to-mass ratio, and relatively high efficiency make AFPM machines an attractive alternative to traditional radial-flux solutions. However, their integration for widespread application remains limited due to challenges in design, manufacturing, thermal management, and control systems, which ultimately also have an economic impact. This article presents a comprehensive and systematic review of AFPM machines, covering key aspects, including topology classification, design methodologies, electromagnetic modelling, optimisation methods, materials and manufacturing processes, and advanced control strategies. A structured, multi-level classification of AFPM machines is presented, incorporating stator and rotor configurations, magnetic circuit structures, winding types, and materials, thereby providing a unified overview of existing designs. Furthermore, the article presents an in-depth analysis of the sizing equations used to calculate and estimate the parameters, approaches to electromagnetic modelling (including the finite element method and magnetic equivalent circuits), and modern optimisation methods based on artificial intelligence. Particular attention is paid to materials science and new manufacturing technologies, such as soft magnetic composites, printed circuit board stators, and additive manufacturing, as well as to thermal management solutions required for high-power-density applications. This work provides a unified reference framework for researchers and engineers and outlines future directions for the development and industrial adoption of AFPM machines.

Keywords: axial-flux permanent-magnet (AFPM) machines; design optimisation; electromagnetic modelling; materials and manufacturing; thermal management; control strategies

Received: 26 May 2026
Revised: 30 June 2026
Accepted: 5 July 2026
Published: 8 July 2026

1. Introduction

The last decade has seen a steady transition toward the use of various electric motors in passenger and specialised ground vehicles. Leading manufacturers and start-ups are striving to develop new technological solutions and improve/optimise existing designs. Among the wide variety of electric motor designs, a large group of permanent-magnet (PM) machines stands out, predominantly used in EVs, where size and weight are important factors. The permanent-magnet disc machine, developed in the 1970s, attracted considerable research attention in the 1980s. Campbell, for example, proposed an axial-field DC machine with a disc-shaped armature in the late 1970s [1,2]. The parameters of this novel motor topology were calculated using a computer program [3], and subsequently, permanent-magnet disc motors were investigated. This group of motors can be divided into two major categories: radial-flux permanent-magnet synchronous motor (RFPMSM) and AFPM synchronous motor (AFPMSM) technologies.

This review article comprehensively and holistically investigates aspects of AFPM motors, as this type of machine is less common and less researched, despite promising characteristics that have attracted increasing practical interest in expanding its use. These days, AFPM motors are becoming more and more attractive options for many applications, including new energy vehicles (alternative power vehicles such as the primarily battery EVs and plug-in hybrid EVs) [4,5], aerospace [6], marine propulsion [7], and other industrial applications [8,9]. Compared with traditional radial-flux permanent-magnet (RFPM) motors, AFPM machines are particularly attractive for compact applications because they provide higher torque and power density while maintaining high efficiency. Their favourable electromagnetic geometry enables efficient utilisation of active materials and improved heat dissipation, whereas modular and scalable configurations further enhance design flexibility. Recent advances in power electronics, magnetic materials, and manufacturing technologies, including additive manufacturing, have mitigated many conventional limitations of AFPM machines, making them promising candidates for next-generation electromechanical systems with enhanced dynamic performance [10].

In parallel with the rapid development of AFPM machines, considerable efforts have also been devoted to conventional radial-flux permanent-magnet machines and other advanced permanent-magnet machine topologies. While RFPM machines remain the dominant and most mature solution for electric drives, recent studies have demonstrated the potential of partitioned stator flux-switching PM machines with strongly coupled flux-reversal effects for transportation electrification [11], as well as hybrid-magnet multilayer interior permanent-magnet synchronous motors (IPMSMs) intended for low-voltage electric truck applications [12]. These developments underline the growing diversity of PM machine technologies and further emphasise the importance of investigating AFPM machines as a promising alternative for high-efficiency and high-power-density electromechanical systems.

To provide a comprehensive and in-depth state-of-the-art overview of the current status of AFPM motors, which is also conducted in slightly different ways by several scientific and engineering groups [13–16], it is important to highlight specific sections in this study, including those that distinguish it from similar articles:

- Literature survey;
- Various novel topological structures of AFPM machines;
- Design and optimisation (sizing equations, electromagnetic modelling and simulation, optimisation design methods, materials and manufacturing processes, and thermal management);
- Overview of control strategies and techniques for AFPM machines;
- Conclusion, research gaps, and future directions.

In these sections, important design factors and characteristics of electric motors are presented and discussed, along with technological solutions that enable comprehensive development in this field.

Regarding topological structures, research primarily focuses on optimising rotor shape, stator design, winding structure, and permanent magnet selection. Research on AFPM machine topologies primarily focuses on rotor and stator configurations, winding structures, and permanent magnet arrangements, with performance commonly evaluated in terms of air-gap flux density, back electromotive force, flux linkage, cogging torque, and torque ripple [17–19]. In addition, design optimisation relies on electromagnetic modelling, advanced materials, manufacturing technologies, and effective thermal management, all of which are essential for improving the performance and industrial applicability of AFPM machines. Due to specific designs, this topic requires special attention.

Furthermore, in terms of control techniques, efforts should be directed toward simplifying the control system architecture and improving the accuracy of control algorithms to achieve superior dynamic performance, high reliability, and robustness [20,21]. In addition, various options are currently being considered for materials that improve motor properties and characteristics or reduce production costs while maintaining similar specifications. For example, changing the composition of magnet alloys, particularly by reducing the concentration of rare-earth elements, reduces dependence on expensive, often imported materials, thereby addressing strategic challenges for the entire manufacturing sector. Also, research is underway to replace the winding material, and copper may be replaced with aluminium.

Unlike many existing review papers that mainly focus on specific aspects of AFPM machines, such as topology, electromagnetic modelling, or control methods, this work combines these topics within a single review and discusses them from the perspective of practical machine development. Particular attention is given to the proposed six-level topology classification, the comparison of sizing approaches and modelling techniques, and recent developments in materials, manufacturing processes, thermal management, and control strategies. Rather than addressing these subjects separately, this review summarises their current state and highlights the main challenges that still limit wider industrial adoption of AFPM machines. The novelty of this review lies in the fact that it provides a structured reference for researchers and engineers involved in the design and optimisation of future AFPM drives and is also organised in a way that makes the main trade-offs easier to compare across topology, modelling, materials, and application constraints. In addition, the conclusions summarise the main research gaps identified from the reviewed literature and outline several future directions that may support further technological development and wider industrial adoption of AFPM machines.

The paper is organised as follows: Section 2 reviews the literature on AFPM motors. Section 3 states the main challenges in this area: torque, flux leakage, demagnetisation, control strategies, materials, and other key issues. Section 4 provides AFPM motor topologies. Section 5 addresses design-optimisation investigations and solutions. Section 6 evaluates control strategies, and Section 7 presents the discussion and conclusions.

2. Literature Survey

In the process of preparing materials and research for this review article, the results of publication activity in key scientific citation databases and publishing houses were also analysed. It is clear that there is a trend toward an increasing number of articles on this topic, and, in recent years, more research groups have been engaged in scientific and technological research related to AFPM motors. To present the results of the publication analysis, the table below shows the databases, keywords, and general metrics by publication type.

In addition, for greater clarity, the number of publications by keywords is given (from Table 1), and several popular publishers on this topic of the automotive industry have been selected: MDPI—166 (115), Elsevier (ScienceDirect)—256 (110), and IEEE Explore—960 (333).

Table 1. An overview of literary sources and databases based on the keywords of this topic.

Scientific Database	Keywords	Type of Publication	Results
Scopus	Axial-flux permanent magnet, topological structure, modelling, optimisation, control techniques (methods)	Article (992) Conference paper (971) Conference review (34) Review (20) Book chapter (5) Book (2) Erratum (1)	**Total amount—2025, The last 5 years—805**
Web of Science		Article (856) Review Article (13) Early Access (5) Editorial Material (2) Correction (1) Proceeding Paper (112 *)	**Total amount—872, The last 5 years—393**

*** not included in the final total amount.**

Consecutively, the literature used in this scientific article was divided into three main periods (Figure 1). Early research conducted before 2000 (approximately 5%) focused on the fundamental principles of axial-flux machines. In the period from 2000 to 2015 (about 27%), research focused mainly on the development of machine topologies and modelling methods. Since 2015, there has been a significant increase in research activity (by about 68%), driven by the rapid development of EV technology and the demand for EVs with high power density.

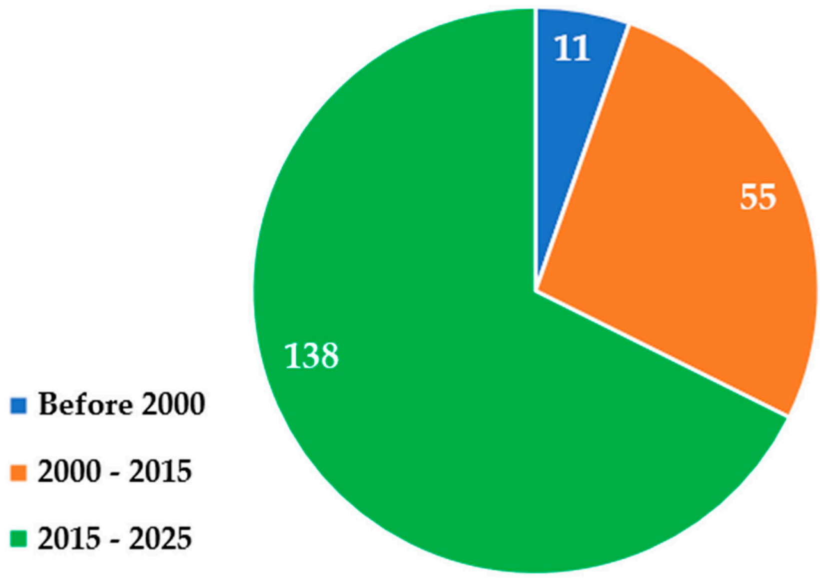

Figure 1. Bibliometric distribution of AFPM-related publications grouped by time periods (before 2000, 2000–2015, and 2015–2025), illustrating the rapid increase in research activity in recent years.

3. Challenges in AFPM Motors

3.1. Mechanical Challenges

A significant amount of mechanical complexity is involved in rotor–stator alignment in AFPMSMs, especially in coreless and dual-rotor systems. Operational stability and reliability can be adversely affected by eccentricity and axial force imbalance caused by assembly-induced misalignments [22]. As a result, to accomplish strict tolerance control, new manufacturing techniques—such as automated assembly procedures and high-precision laser-based alignment—are needed, particularly in architectures that use segmented stator structures or Halbach magnet arrays [23].

3.2. Cogging Torque and Torque Ripple

Axial-flux motors have a planar magnetic flux path, which increases cogging torque and torque ripple, thereby reducing control accuracy and acoustic performance [24]. Despite their effectiveness, mitigation strategies such as magnet skewing, fractional-slot winding configurations, and auxiliary slotting often come with trade-offs, such as lower power density or greater structural and manufacturing complexity [25]. As a result, there remains a substantial research gap in developing reliable multi-objective optimisation techniques that can concurrently optimise torque smoothness, efficiency, and manufacturability across a variety of AFPMSM topologies.

3.3. Flux Leakage and Demagnetisation

AFPMSMs are vulnerable to irreversible demagnetisation and flux leakage, especially in high-load or high-temperature environments. Halbach arrays increase flux concentration, but they also introduce cost inefficiencies and production complexity [22,26]. Understanding the dynamic demagnetisation characteristics of rare-earth magnets under transient or fault conditions, which are crucial for automotive and aerospace applications, remains limited.

3.4. Control Strategies and Limitations

AFPMSMs lag behind radial-flux motors in fault-tolerant methods and sensorless control [25]. Fault detection in multi-phase systems and position estimation at low speeds are still difficult, especially in encoderless applications. Although they require further experimental validation, emerging methods, such as machine-learning-based diagnostics and high-frequency signal injection, show promise.

3.5. Manufacturing and Material Exploitation

The most important goals of motor design optimisation are lightweighting and performance enhancement. Additionally, the mechanical robustness of lightweight coreless designs remains a significant challenge, underscoring the value of ongoing research into complex composite materials and modular structural approaches. Furthermore, the thermal behaviour of novel materials, such as soft magnetic composites (SMCs), under high-frequency operation remains underexplored.

3.6. Difficulties in Thermal Management

Because AFPMSMs have high power density, they generate concentrated heat in a limited axial region, rendering traditional radial cooling techniques ineffective [27]. This research suggests axial cooling channels or integrated liquid-cooling systems, but these solutions need to be validated using multiphysics simulations that combine electromagnetic loss models with computational fluid dynamics (CFD) [27].

3.7. Diversification and Application in Various Fields of Industry

As is well known, AFPM motors are currently limited to a narrow range of vehicles, and in cars, they are primarily used in premium, sports, or deep-specialised segments. In addition to technical and engineering challenges, this also poses challenges for the commercial and social spheres, expanding the possibilities for introducing these types of motors into broader segments of consumer passenger transport. The issues of optimisation, both in the production process and in the use of materials, raised above, have a direct

https://doi.org/10.3390/app16146854

impact on the solution to this problem. Several scientific projects are already working on this and are seeking to solve this problem [28].

This paper advances the development of high-efficiency AFPM motors by systematically examining achievements, performance results, technological solutions, and material choices in manufacturing.

4. Topology of AFPM Motors: Systematic Structure

A wide variety of AFPM motor topologies have been proposed, and several publications describing different types were reviewed [29–34] to analyse designs. Some authors provided a wide range of topological structures implemented in a single summary scheme [16,35]. On the other hand, the current review article applies a more thorough, modular approach, including categories and levels.

The classification of AFPMSM topologies can be represented using six levels:

The first level divides AFPMSMs into four types based on the number of stators and rotors [36]: single-stator single-rotor (SSSR), single-stator double-rotor (SSDR), double-stator single-rotor (DSSR), and multi-stator multi-rotor (MSMR) [29]. AFPMSMs can also be classified based on magnetic structure topology, such as axial-flux internal rotor (AFIR) and toroidal stator (Torus).

The second level distinguishes AFPMSMs based on their magnetic topology. Representative topologies include axial-flux internal rotor (AFIR), axial-flux outer rotor (AFOR), toroidal stator (Torus), and yokeless and segmented armature (YASA) configurations. These topologies differ in magnetic flux paths, structural arrangement, and performance characteristics.

To facilitate understanding, detailed block diagrams illustrating the topology of the main types of AFPM motors have been prepared in Figure 2, which shows the classification of topologies and the construction of AFPMSMs.

The third level classifies structures as iron-core and coreless. Iron-core machines contain ferromagnetic material in the stator and generally provide higher torque density, whereas coreless machines eliminate stator iron, reducing cogging torque and iron losses [30].

The fourth level classifies the stator-slot structure as slotted and slotless configurations [31]. Slotted machines provide improved magnetic coupling and torque capability, while slotless designs reduce torque ripple, acoustic noise, and cogging effects. Coreless machines are inherently slotless.

The fifth level classifies AFPMSMs into parallel “NN” and series “NS” magnetic circuit structures. The relative orientation of magnetic poles across the air gap in electric machines with multiple air gaps (SSDR, DSSR, and MSMR) is determined by the pole-polarity configuration. In the “NN” configuration, identical poles face each other, causing magnetic repulsion that reduces effective air-gap flux density and increases leakage flux, though it can improve mechanical stability and reduce axial forces. By contrast, the “NS” configuration aligns opposite poles, creating a strong flux path across the air gap and enhancing magnetic attraction, air-gap flux density, and torque or force production.

At the sixth level, AFPMSMs are classified into different winding arrangements. A winding structure called “drum winding” surrounds the stator in the radial and circumferential directions. Another option is toroidal winding, which wraps around the stator in both radial and axial directions and is always non-overlapping, as shown in Figure 3. Other winding types include concentrated, distributed, PCB, and hairpin windings. All of these winding types affect the winding factor, manufacturability, cooling capability, and achievable power density of AFPMSMs [32].

https://doi.org/10.3390/app16146854

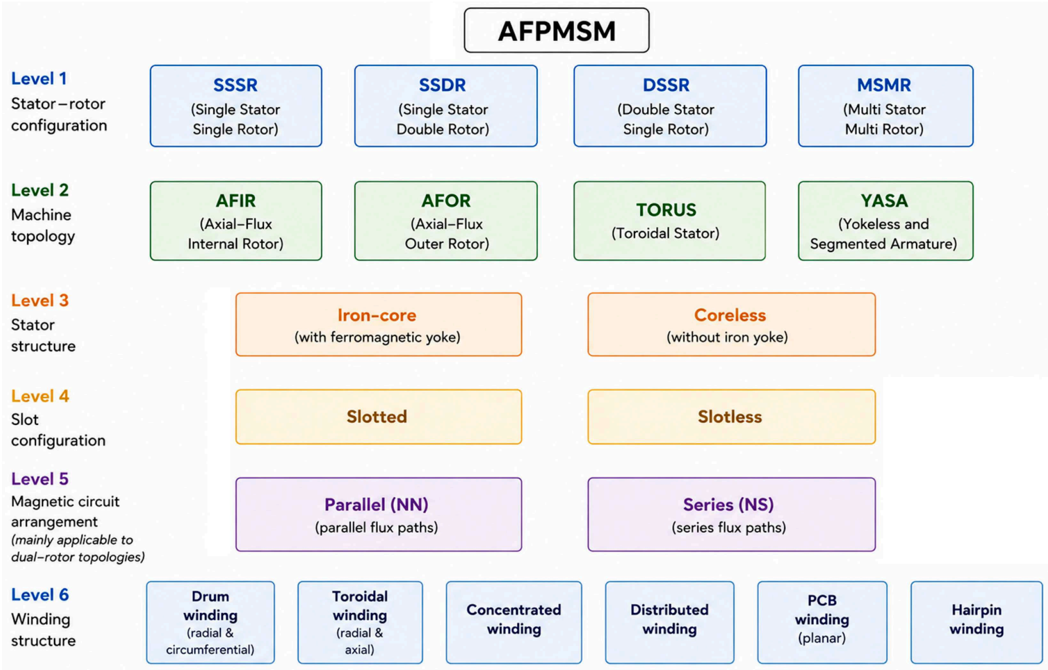

Figure 2. Six-level hierarchical framework for the classification of axial-flux permanent-magnet synchronous motors. The framework summarises the principal stator–rotor configurations, machine topologies, stator structures, slot configurations, magnetic circuit arrangements, and winding structures used in AFPMSMs. Note that levels represent independent classification coordination. The combinations among the options across different levels are possible.

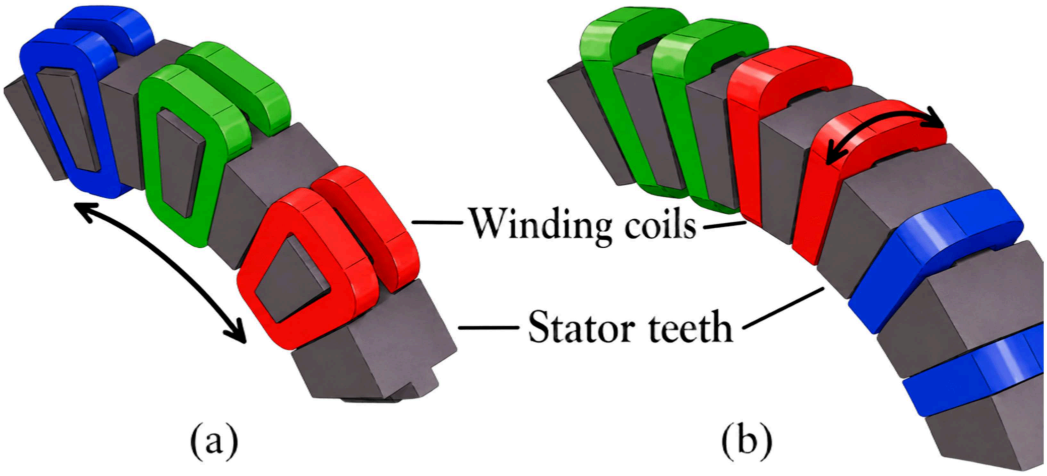

Figure 3. Schematic illustration of the three-phase winding structure for AFPMSMs—drum (**a**) and toroidal (**b**). Arrows indicate the winding direction of the concentrated coils around the stator teeth. (based on [15]).

Unlike most existing classifications, which are usually limited to a single design aspect, such as stator–rotor arrangement or machine topology, the proposed framework introduces a six-level hierarchical structure that combines electromagnetic topology, stator architecture, slot configuration, magnetic circuit arrangement, and winding technologies. Since each level represents an independent classification dimension, different combinations can be described systematically, providing a more comprehensive and extensible representation of AFPMSM designs. This approach facilitates the comparison of existing machines and offers a structured basis for future topology development and design optimisation.

The SSSR motor, which consists of a stator with a winding, an iron disc, and a rotor formed of a steel disc, is the most basic structural configuration. Because there is only one air gap, the rotor produces a significant axial force on the stator, which could cause mechanical damage if the design or assembly is insufficient. Furthermore, the rotor's alternating magnetic field within the stator increases magnetic losses, thereby lowering the motor's overall efficiency. As a result, SSSR motors have not been widely used in practical applications.

In SSDR-type and AFPM motors with a toroidal stator (Torus), the stator between the two rotors provides a symmetrical structure that effectively balances axial forces. In general, this symmetry helps reduce vibration and enhances motor durability throughout its operational lifespan. Slotless machines experience less copper loss and improved heat dissipation due to their shorter end windings. Additionally, by reducing leakage and mutual inductance, this configuration eliminates slot-related problems such as cogging torque, flux ripple, high-frequency rotor losses, and stator tooth problems.

Mostly, this type of motor is a Torus. As seen in Figure 4, the Torus motor's stator is placed between two permanent-magnet rotors formed by steel discs with NdFeB permanent magnets and a shaft. There are two types of Torus motors: slot (torus-S) and slotless (torus-NS). With its straightforward stator construction, low motor leakage inductance, and minimal torque fluctuations, the torus-NS motor performs effectively, but it requires more permanent magnets, which increases production costs [33].

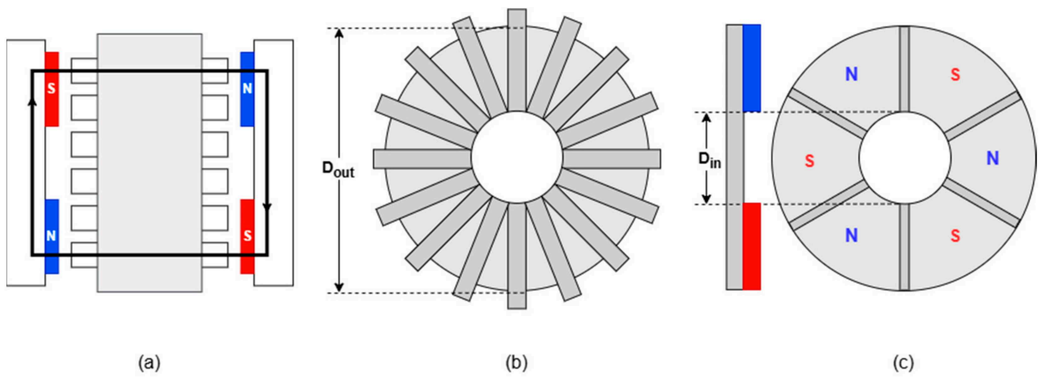

Figure 4. Schematic illustration of the Torus-NS motor structure with magnetic circuit (**a**), stator (**b**), and rotor structure (**c**). The blue and red colours correspond to the PM poles.

Based on the shape of the magnetic circuit, Torus-S motors can be further divided into "NN" and "NS" types [26,27]. The two rotors of the "NN" type Torus-S motor have homopolar magnetic poles, as seen in Figure 5a. With the air gap, windings, and a portion of the stator core on this side, the N and S magnetic poles on both sides of the rotors generate a parallel magnetic circuit. When the stator core is thick enough, the two parallel magnetic circuits flow through it circumferentially without interfering with one another.

The two rotors of the "NS" type Torus-S motor have heteropolar magnetic poles, as seen in Figure 5b. With the air gap and windings on this side, the N and S magnetic poles on either side of the rotors generate a series magnetic circuit that axially penetrates the stator core.

In DSSR-type AFPM motors, where the rotor is positioned between two stators, the PM is either inside or on top of the rotor. Embedding the PM inside the rotor offers better protection against impact and corrosion than surface placement [34]. DSSR AFPM machines have a relatively high copper loss due to their long end windings. A slotted stator design exhibits lower copper losses than a slotless structure, thereby improving efficiency [37].

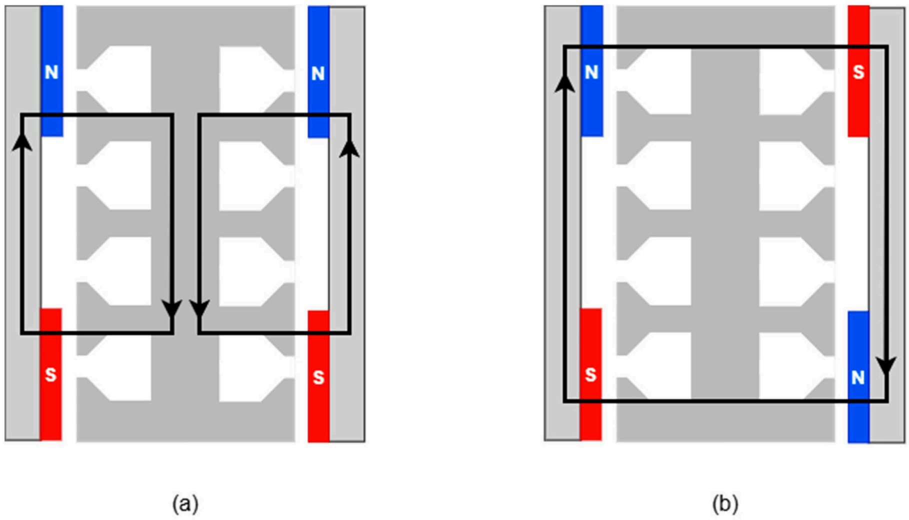

Figure 5. Schematic illustration of the magnetic circuit structure of the Torus S motor. NN (**a**) and NS (**b**) types. The blue and red colours correspond to the PM poles.

An intermediate rotor and two stators mounted on either side of the rotor form a dual-stator single-rotor AFPMSM with an axial-flux internal rotor (AFIR) design. The AFIR motor's two stators create a revolving magnetic field. As a result, it has a broader high-efficiency coverage and more flexible control. Thus, it is necessary to investigate a continuous, stable, and highly effective control method for AFIR motors [38]. In contrast to a Torus motor, the AFIR motor's rotor is composed of axially magnetised NdFeB permanent magnets and a shaft without a steel disk. Non-magnetic materials are used to fill the gap between the magnets to create a rigid framework that can support the magnets without a rotor disc [39], as seen in Figure 6.

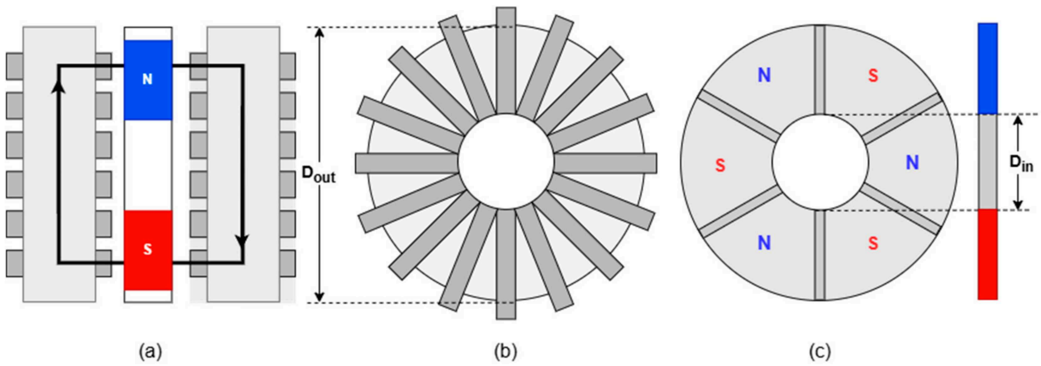

Figure 6. Schematic illustration of the AFIR-NS motor structure with the magnetic circuit (**a**), stator (**b**), and rotor structure (**c**). The blue and red colours correspond to the PM poles.

The permanent magnets can be mounted either on the rotor surface or embedded within it. Compared with surface-mounted magnets, embedded magnets offer better protection against mechanical impact and corrosion. AFIR motors come in two varieties: slotless (AFIR-NS) and slotted (AFIR-S). The construction of an AFIR-S motor is depicted in Figure 7 [40].

The rotor of the AFIR motor with magnetic circuit type "NS" often lacks a steel disc. However, other experiments have separated the rotor's steel disc into two sections and positioned permanent magnets facing the stators on both sides to create an "NN" type magnetic circuit, facilitating control.

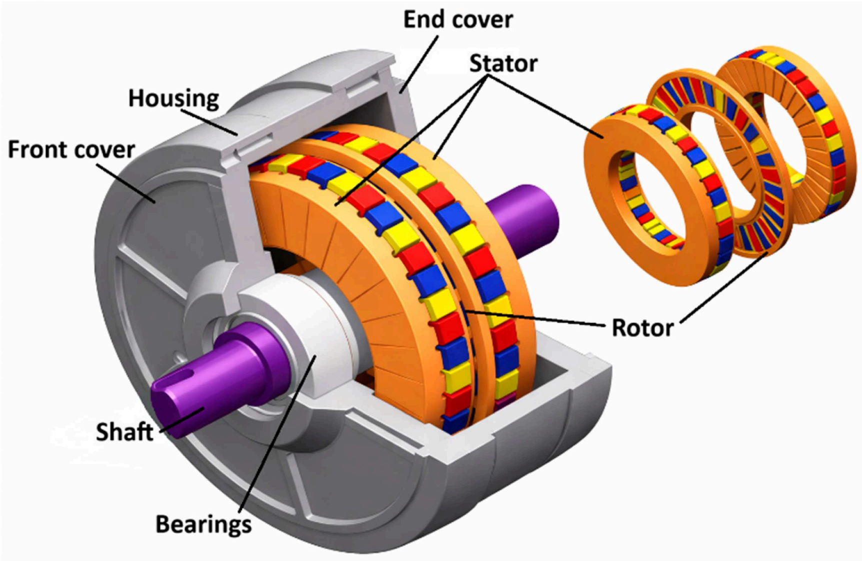

Figure 7. Adapted Schematic illustration of the AFIR-S motor structure with its components [15].

MSMR-type AFPM

A multi-disc motor consists of N stators and (N + 1) rotors. Multiple stacked AFIR and torus-structure motors combine to form this type of motor. The MSMR motor typically increases the disc diameter to enhance motor torque [41]. However, the torque can only be increased to a certain degree due to the constraints of the axial force applied by bearings and the rigidity of the disc. For high-torque transmission systems, a multi-disc motor is therefore an excellent alternative. Additionally, the number of stators can be increased to enhance the motor's output power because the power of an AFPMSM is independent of its axial length [42]. This configuration significantly increases torque and power density without enlarging the motor diameter, making it particularly suitable for high-torque applications such as ship propulsion.

The advantages and disadvantages of different AFPMSM structures, as well as typical torque (power) density with performance basis, according to the number of stators and rotors, were discussed in the Sections above, and Table 2 provides an overview.

Table 2. Comparison of advantages and disadvantages of major AFPM machine topologies.

Structure	Advantages	Disadvantages	Typical Torque (Power) Density	Performance Basis	Ref.
SSSR	Simple and robust structure; low cost; good cooling capability	High axial-flux imbalance; high axial force; increased flux leakage; limited electromagnetic utilisation	Low–Medium <30–40 kNm/m^3	A single air-gap configuration limits magnetic flux interaction and active torque-producing area.	[43–46]
SSDR	Smoother torque production; balanced axial forces; improved flux utilisation	Increased mechanical complexity; higher rotor inertia; higher manufacturing cost	High 40–70 kNm/m^3	The dual-rotor structure creates two active air gaps, increasing electromagnetic interaction.	[47–49]

Table 2. *Cont.*

Structure	Advantages	Disadvantages	Typical Torque (Power) Density	Performance Basis	Ref.
DSSR	Enhanced magnetic coupling; reduced leakage flux; high efficiency potential	Increased stator mass, more complex cooling, higher cost and assembly complexity	Very High 70–100 kNm/m^3	Dual stators maximise active electromagnetic surfaces and improve torque generation capability.	[50–54]
Torus-NS	Very low torque ripple and acoustic noise; reduced core losses	Lower overload capability; complex winding; higher manufacturing cost	Medium ~40 kNm/m^3	A slotless toroidal structure reduces losses and ripple but limits magnetic loading.	[55–59]
Torus-S	Improved magnetic flux concentration; compact construction	Increased torque ripple; more complex stator manufacturing	High 40–70 kNm/m^3	Slotted toroidal stator enhances air-gap flux density and electromagnetic loading.	
AFIR	Compact and mechanically protected rotor; fast dynamic response	More difficult thermal management (at high load); complex assembly and maintenance	Very High 70–100 kNm/m^3	The internal rotor configuration enables efficient use of the active radius and a compact electromagnetic design.	[23,47,57,60]
Multi-disc (MSMR)	Scalable for high-power applications; very high output capability	Difficult cooling implementation; high manufacturing and control complexity	Extremely High >100 kNm/m^3	Multiple active rotor–stator interfaces significantly increase the total torque-producing area.	[23,47,61–63]

Note: Typical torque (power) density marks are qualitative comparisons summarised from the reviewed literature and representative AFPM machine configurations.

The wide variety of AFPM machine configurations demonstrates that no single topology is universally optimal. In general, higher torque density and improved electromagnetic utilisation achieved by dual-rotor, dual-stator, and multi-disc arrangements are accompanied by increased manufacturing complexity and more demanding thermal management. Conversely, simpler structures offer easier implementation and lower cost at the expense of output capability. Therefore, AFPM machines can be tailored to specific requirements and applications by balancing dimensional constraints, weight, power density, torque capability, manufacturability, and cooling requirements, rather than by maximising a single performance index.

5. An In-Depth Investigation of Design Optimisation

For the progressive, methodical design of AFPM motors, the first stage typically begins with size constraints and performance requirements to analyse all relevant aspects. Then, the selection and optimisation of key parameters begin, followed by the final preparatory stage, in which the mechanical characteristics of the entire design are evaluated [29,64,65]. Typical design and analysis methods for AFPM motors were developed over many years of research in academic and industrial settings. This section discusses various approaches to dimensioning and summarises the latest developments in electromagnetic modelling equations, AFPM motor-design optimisation, and simulation modelling. It also presents a mathematical comparison method for axial and radial motors that accounts for similarities in characteristics and requirements.

5.1. Sizing Equations

To achieve the required power/torque characteristics within the specified limitations (e.g., maximum permissible geometric dimensions, rated/peak torque, rated/peak speed, peak voltage/current, etc.), the design process begins by determining the external dimensions of AFPM motors [66,67]. Equation (1) can be used to determine the output power of AFPM motors P_{out}. If the stator resistance and leakage inductance are minimal, these values can be neglected [68,69]. Here, η is the motor efficiency; n_p is the number of motor phases; T is the periodic cycle of the motor electromotive force (EMF); $e(t)$ is the phase air-gap EMF; $i(t)$ is the phase current; $\mathrm{K_p}$ is the electrical power waveform factor; and $\mathrm{E_{pk}}$ and $\mathrm{I_{pk}}$ are the peak values of phase air-gap EMF and phase current, respectively:

$$P_{out} = \eta \frac{n_p}{T} \int_0^T e(t) i(t) dt = \eta n_p K_p E_{pk} I_{pk} \tag{1}$$

where $\mathrm{K_p}$ and $\mathrm{E_{pk}}$ can be defined from ref. [70]:

$$K_p = \int_0^T \frac{e(t) i(t)}{E_{pk} I_{pk}} dt \tag{2}$$

$$\mathrm{E_{pk}} = \mathrm{K_e N_{ph} B_g} \frac{f}{p} (1 - \lambda^2) {D_o}^2 \tag{3}$$

where $\mathrm{K_e}$ is the EMF factor per unit air-gap area; $\mathrm{N_{ph}}$ is the number of windings turns per phase; $\mathrm{B_g}$ is the flux density in the air gap; f is the electrical frequency; p is the motor pole pairs; and l is the ratio of the inner diameter D_i to the outer diameter D_o of the motor.

By combining all of the equations presented above, researchers [71] derived a general size equation. Here, $\mathrm{K_\phi}$ is the ratio of electrical load on rotor and stator; n_1 is the number of phases of each stator; $\mathrm{K_i}$ is the current waveform factor; $\mathrm{K_L}$ is the aspect ratio coefficient related to the motor structure, considering such factors as energy consumption loss, temperature rise and demand efficiency; A is the total electrical load; $\mathrm{L_e}$ is the effective axial length of the motor; and $\mathrm{K_L} = \mathrm{D_o}/\mathrm{L_e}$.

$$P_{out} = \frac{1}{1 + \mathrm{K_\phi}} \frac{n_p}{n_1} \frac{\pi}{2} \mathrm{K_e K_i K_p K_L}\ \eta \mathrm{B_g} A \times \frac{f}{p} (1 - \lambda^2) (\frac{1 + \lambda}{2}) {D_o}^2 \mathrm{L_e} \tag{4}$$

Other researchers proposed their own approach to size determination using specific equations [72]. Equations for electric motor sizing (both axial and radial flux) correspond the machine's output to the dimensions of the motors as well as the design parameters of electric loading $\hat{A}$ and magnetic loading $\hat{B}_\delta$. The electromagnetic torque of electric machines can be computed by integrating the air-gap field quantities generated by the electric and magnetic loading using the Maxwell stress tensor, as shown in ref. [72]. In contrast to RFPM motors, an AFPM motor does not have a single air-gap radius. This introduces complexities in determining the proper radius r to specify the electric loading for an AFPM. The electric loading will not be identical at any radius because the air gap expands radially. Consequently, it is necessary to consider the electric loading $\hat{A}$ as a function of the radius $r \in [R_{in}, \mathrm{R_{out}}]$ (Figure 8).

Researchers [73] have provided a comprehensive derivation of the AFPM motor sizing equation that accounts for the electric loading as a function of radius. This equation can be presented in terms of the geometric ratio $\lambda = \frac{\mathrm{R_{in}}}{\mathrm{R_{out}}}$ for the coreless and single-sided AFPM:

$$T = \frac{\pi}{2} \hat{B}_\delta \hat{A} R_{out}^3 \lambda (1 - \lambda^2) \tag{5}$$

where T is the electromagnetic torque, R_{out} is the outer air-gap radius, and L is the axial length. The AFPM motor's electromagnetic torque is observed to vary with the cube of its outer radius, and the geometric ratio λ is once more a crucial design factor. For power-dense designs, the range $\lambda \in [0.65, 0.75]$ has been described [74].

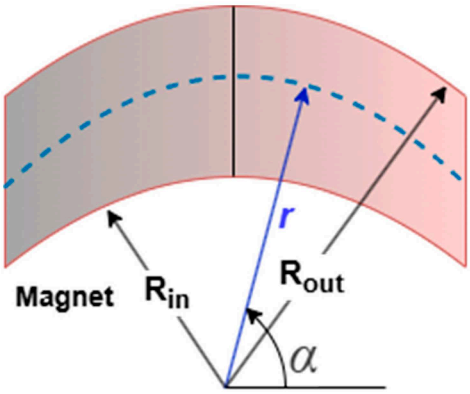

Figure 8. The basic radial dimensions of AFPM motors.

These two sizing Equations (3) and (5) are based on similar geometric and electromagnetic assumptions and describe the same active zone of an axial electric motor. Both the use of the parameter λ, which establishes the radial ratio of the active area, and the presence of the multiplier $(1 - \lambda^2)$, which characterises the effective working area, show how comparable they are. The fact that the output characteristics in both situations are highly correlated with the magnetic induction in the air gap highlights their common electromagnetic basis. The difference between the equations is due to the physical nature of the calculated quantities. Equation (5) describes the electromagnetic torque and scales with the cube of the characteristic radius, reflecting the force nature of the interaction. Equation (3) determines the output power and scales with the area of the active zone and frequency, which corresponds to the energy description of the electromechanical conversion process. Thus, these equations are complementary and together provide a comprehensive picture of the power and energy capabilities of an axial electric motor at the preliminary design stage.

Therefore, in AFPM motors, the diameter ratio λ is a crucial design element that significantly affects their performance characteristics [75]. Researchers demonstrated that the diameter ratio λ directly controls the power density of AFPM motors for a given number of pole pairs, reaching a maximum at a certain value [76]. However, the ideal diameter ratio in real-world applications varies with the optimisation objective. The ideal value of λ changes with rated power requirements, the number of pole pairs, and the motor topology, even when the electrical loading and magnetic flux density are the same [77,78]. Furthermore, experiments reported in ref. [79] indicated that the rational selection of key parameters—such as magnetic flux density, electrical loading, and current density—enables accurate estimation of the primary geometric dimensions of AFPM motors. This approach facilitates effective parameter matching and supports subsequent design optimisation and performance analysis of AFPM machines.

5.2. Comparison of Design Variants (AFPM—RFPM)

Numerous reports have compared axial-flux and radial-flux permanent-magnet machines. Researchers in ref. [71] examined the power density characteristics of toroidal AFPM, double-stator AFPM, and RFPM designs, revealing that both axial-flux configurations demonstrate higher power density than the radial-flux machine. Furthermore, investigations by Taran et al. [80] and Nishanth et al. [81,82] indicated that single-sided AFPM motors produce similar torque levels when the permanent-magnet volume is held constant. This finding suggests that the single-sided AFPM motor configuration reduces the amount of active material, which minimises manufacturing costs and provides about double the torque per unit rotor volume.

To provide a complete comparison, it is important to derive a dimensional equation for the radial motor as well. To do this, refer to ref. [72], where T is the electromagnetic torque, R_o is the air-gap radius, and L is the axial length.

$$T = \pi L \hat{B}_\delta \hat{A} R_o^2 \tag{6}$$

These sizing Equations (5) and (6) can be used to compare the torque capability of single-rotor single-stator AFPM and RFPM designs for different RFPM rotor aspect ratios. Combining these equations, the following equation can be derived:

$$\frac{T_{afpm}}{T_{rfpm}} = \frac{\frac{\pi}{2}\hat{B}_\delta \hat{A} R_{out}^3 \lambda(1-\lambda^2)}{\pi L \hat{B}_\delta \hat{A} R_{out}^2} = \frac{D_{out}\lambda(1-\lambda^2)}{4L} \tag{7}$$

where $D_{\text{out}} = 2R_{out}$ is the outer diameter of the AFPM and RFPM rotors, and $\frac{D_{out}}{L}$ is the aspect ratio of the RFPM rotor.

The torque per rotor volume (TRV) is also useful for comparing RFPM and AFPM systems. Considering Equation (6), it might be expressed that TRV for RFPM designs is given by $\text{TRV}_{rfpm} = \hat{A}\hat{B}_\delta$, and the TRV for AFPM motors can be computed as $\text{TRV}_{afpm} = \frac{\lambda R_{\text{out}}}{2(t_m+t_y)}\hat{A}\hat{B}_\delta$. In the majority of effective designs, AFPM designs have a greater TRV than RFPM designs because of the combined thickness of the PM and rotor yoke $t_m + t_y < \frac{\lambda R_{\text{out}}}{2}$.

The torque per PM volume (T_{PM}) as a further significant indicator for comparing axial- and radial-flux PM machines. To lower system costs and avoid supply chain problems when obtaining PMs, most drive systems should reduce PM volume. Using Equations (7) and (8), the torque-to-PM-volume ratio can be calculated to compare radial- and axial-flux topologies. The RFPM and AFPM variations are assumed to have the same outer radius, air-gap length, and electric and magnetic loading in Equation (8). For every machine that can be physically realised, $\lambda < 1$ and $t_m < D_{out}$.

$$\frac{T_{PM,afpm}}{T_{PM,rfpm}} = \frac{D_{out}\lambda(1-\lambda^2)}{4L} \times \frac{\pi\left(R_{out}^2 - (R_{out}-t_m)^2\right)L}{\pi R_{out}^2(1-\lambda^2)t_m} = \lambda(1 - \frac{t_m}{D_{out}}) \tag{8}$$

This suggests that AFPM motors require a higher PM volume than comparable RFPM motors to achieve the same torque output.

5.3. Electromagnetic Modelling

Electromagnetic modelling of an AFPM motor is an important step in electric motor analysis, following the definition of the dimensional equation, and serves as the basis for optimising the AFPM design and evaluating performance [83]. The methods for creating an electromagnetic model and analysing the electromagnetic characteristics of AFPM motors include two main approaches: finite element analysis (FEA) [84–86] and magnetic equivalent circuit (MEC) [60].

The core concept of the magnetic equivalent circuit is to simplify the complex magnetic field by treating it as a simple circuit. Compared with FEA, MEC is considered a simpler method for analysing the electromagnetic models and performance of AFPM motors [32].

The MEC technique analyses and solves magnetic-field problems using circuit theory. The magnetic circuit can be weakly or strongly linked to the machine geometry, leading to simple [87,88] or very complex [89,90] grid-like circuits, which, in extreme cases, are similar to finite element meshes. In most situations, however, the circuit is of medium complexity, as seen in other works [91,92], with nodes defined for individual sub-zones of the machine and the nearest nodes linked via wires. Lumped resistors (reluctances) indicate the magnetic conductivity of materials and media, whereas voltage sources represent the magnetomotive force of magnets and coils. The dimensions and resolution of the entire circuit can vary within a single model, depending on the flexibility with which the equivalence between the real geometry and the circuit can be defined. Additionally, without converting to a linear equivalent machine, the MEC can directly represent the ring shape of the AFPM motor as a 2D circuit, a multi-slice 2D circuit, or a 3D circuit if the reluctances are characterised as segments [88]. The MEC technique allows the use of nonlinear reluctances, which are very simple to calculate using circuit theory, to model the ferromagnetic properties of soft magnetic cores. Furthermore, inductances in the magnetic circuit can be used to simulate even dynamic behaviour. By modelling eddy-current or hysteresis effects, these magnetic inductances can be solved dynamically in the MEC, directly accounting for reaction-field effects [93]. Also, an electrical circuit linked to the MEC can represent the eddy-current effect based on the geometry of a cross-section [94,95]. Therefore, the MEC has significant potential for accurately and dynamically modelling the behaviour of soft magnetic materials. On the other hand, using MECs to represent low-permeability zones, such as air or PMs, is more difficult than using Fourier-based analytical models, for example. These zones can still be accurately modelled using a variety of techniques, including flux tubes [92,96,97], conformal mapping [91], and high-resolution MEC networks [98,99]. However, the last option incurs a higher computational cost, while the first two require prior knowledge of the field directions. Finally, another problem is the relative motion between the stator and rotor, which can be resolved by interpolating on a sliding interface [98], gradually modifying the values of the air-gap reluctances [92,96], and reconnecting wires stepwise or zone-wise [99]. As an alternative, the circuit remains identical, while the rotor circuit components are configured to switch their characteristics to simulate motion [89].

In conclusion, MECs can compute target variables, account for specific effects, and provide a wide range of functionalities, including dynamic material behaviour. To determine the strategy with the greatest precision and computational efficiency, the various options for modelling the air gap and movement should be compared and assessed uniformly. From an engineering perspective, MEC models are particularly suitable for preliminary design studies and sensitivity analyses because they provide rapid evaluation of machine characteristics while retaining acceptable accuracy. However, their predictive capability becomes increasingly dependent on the representation of leakage flux paths and air-gap regions, which limits their use for detailed local-field analysis.

5.4. Numerical Simulation FEA (2D FEA and 3D FEA)

With 2D FEA, all target AFPM motor quantities may be computed, except the end winding components of the AC winding losses and the exact eddy current. For the transient winding loss calculation, only radially oriented conductors can be modelled in the cylinder surface, the same as in ref. [100]. Nevertheless, there is no confidence that the magnetic field at the radial ends would resemble the field that exists in the windings between two neighbouring stator teeth. The winding loss computation may become inaccurate as a result. Additional models in refs. [101,102] should be applied, along with the magnetic simulation to model eddy currents, particularly in solid, conductive PMs. Apart from the objective quantities, the ability to model the unique impacts of the AFM for several 2D FEA methods is investigated.

Initially, the single-slice 2D FEA is analysed using analytical extensions, as reported by Sun et al. [103]. The 2D model accounts for saturation but not for radial changes in saturation. The radial tooth tips, the corresponding radial field components, and the radial notch effects cannot be included in this method, even though the radial change in the outer contours of the active components, such as the PMs, can be simulated. Additionally, neither the radial overhang nor the radial end-effects are accounted for. The basic multi-slice 2D FEA was been explained in ref. [104] and reviewed. Although it shares many characteristics with the single-slice 2D FEA with analytical extension, discrete slices allow radial modelling of various saturation levels. However, radial field components, radial notch effects, and radial end effects are not simulated because the slices are not linked. Therefore, an extension is proposed in ref. [105] to account for radial end effects using an analytical function like those used in the section on analytical models. Another development is proposed in ref. [106], where a steady field result in the radial direction is obtained by interpolating between radial adjacent slices. To build leakage channels at the radial ends, account for radial notch effects, and allow magnetic flux to enter the radial tooth tips, radial field components are modelled at this level. These methods make the 2D multi-slice FEA methodology an attractive choice by extending its applicability and gradually simulating the entire capabilities of 3D FEA with less computational effort.

The most used electromagnetic modelling simulation technique for AFPM motors is 3D FEA. 3D FEA is the primary method in about 45% of publications, and another 45% use it to validate other simulation techniques. This is because 3D FEA can obtain all target values and estimate all special effects of AF motors. The main disadvantage of this approach remains the computational cost, particularly when all effects and targets are accounted for in a time-stepping dynamic simulation. Although the magnetic vector potential is the dependent variable in most 3D FEAs, methods exist to significantly reduce simulation time by using the magnetic scalar potential in both the coil and magnet regions, as shown in refs. [107–109]. However, in a postprocessing phase, all time-dependent effects and losses must be computed using alternative techniques. The field reconstruction method is another approach for accelerating 3D FEA. The magnetic field distribution from a few finite-element simulation steps is replicated using the geometrical symmetry and periodicity, as well as the time-based periodicity of the AFPM motors [110,111]. Using both of those techniques can result in an acceleration of one or two magnitudes, increasing 3D FEA suitability for axial-flux motors.

Despite its high computational cost, 3D FEA remains indispensable for validating final designs and investigating local electromagnetic effects that cannot be accurately captured by simplified models. Consequently, practical AFPM motor development often relies on a multi-stage procedure in which simplified analytical or equivalent-circuit models are used during the initial stages, whereas detailed FEA is reserved for final verification.

5.5. Optimisation Design

Reliability, cost, and performance must all be carefully evaluated while designing AFPM motors. Consequently, the motor's ideal design is a multi-variable, multi-mode problem [112]. Studies typically begin with the key parameters for the optimal design of AFPM motors and use optimisation algorithms to refine the critical parameters. Common optimisation algorithms include neural networks (NN) [113], genetic algorithms (GA) [114], and least squares (LS) [115]. Meo et al. [116] presented a novel hybrid strategy that combines artificial neural networks (ANN) and multi-objective particle swarm optimisation. A preliminary design based on the sizing equations was created in order to generate the ANN training and verification datasets. Additionally, the algorithm's FEA for various values was developed. The input layer, hidden layer, and output layer of the ANN model have five, fifteen, and one neuron, respectively. The input layer of the ANN incorporates the principal geometric and design parameters that define the structure and electromagnetic

https://doi.org/10.3390/app16146854

configuration of the AFPM machine. These parameters include the number of stator turns (Ns), the number of rotor elements (Nr), the stator tooth width (Wts), the rotor tooth width (Wtr), the permanent-magnet width (WPM), and the stator winding window width (Wo). Together, these variables determine the machine's main geometric proportions and strongly affect the electromagnetic field distribution, magnetic flux paths, and the motor's torque production capability. Variations in these parameters lead to significant changes in the machine's operational characteristics, including efficiency, torque generation, and electromagnetic behaviour. The ANN's output layer represents the predicted performance indicators of the AFPM motor, obtained through the learning process. These outputs include efficiency (η), magnetic flux density (B), electromagnetic torque (C), output voltage (V), and total harmonic distortion (THD). These quantities describe the key electromagnetic and energy performance characteristics of the machine and are typically used as objective functions or evaluation criteria in the optimisation process. By establishing a nonlinear mapping between the design variables and the resulting performance metrics, the trained ANN model enables rapid prediction of motor characteristics and significantly reduces computational cost compared to repeated FEM simulations. To determine the highest torque density and the minimum cogging torque, Fard et al. presented a hybrid approach based on an ANN and the non-dominated sorting genetic algorithm II (NSGA II) [117].

To identify the optimal parameter combination, Patel et al. [118] proposed using GA to optimise the diameter ratio, air-gap flux density, and current density in the design of AFPM motors for EVs. The 3D-FEA model was used to validate the optimised design combination, and the results showed that the AFPM motor's efficiency could reach 91.5%. A hybrid genetic algorithm (HGA) that combines simulated annealing and father-offspring selection [119], the elitist genetic algorithm (EGA) [120], the non-dominated sorting genetic algorithm (NSGA-II) [121], and other hybrid algorithms with GA have also been applied in some studies to optimise the design of AFPM motors.

Considering a specific drive cycle, Sun et al. investigated the analysis, design, and optimisation of a PMSM intended for an EV specified for campus patrol [122]. The rated power and speed range for the PMSM are first determined by dynamic calculations using data such as characteristics and speed obtained from a test EV on campus roads [123]. After that, some basic design parameters and a first design are developed. An optimisation procedure is then carried out to improve the planned PMSM's performance [124]. This includes enhancing the stator core shape, air-gap length, and PM structure shown in Figure 9. To accomplish several objectives simultaneously, a variety of optimisation techniques are implemented, all of which are evaluated using FEA with the corresponding cycles.

New multi-objective optimisation algorithms, including particle swarm optimisation (PSO) [125], bat optimisation (BO) [126], and the Taguchi algorithm [127], have been used to improve the design of AFPM motors. Rostami [128] designed an AFPM motor for EVs using quasi-3D and PSO algorithms, assessing the impact of driving cycles (NEDC and US06) on machine parameters. The 3D finite element model was used to evaluate the reliability of the AFPM motor's design characteristics optimised for different driving cycles, which can vary significantly. Chakkarapani et al. [129] presented three multi-objective optimisation strategies for the design and analysis of slot-less permanent-magnet brushless DC motors: the weighted-sum method (WSM), the multi-objective genetic algorithm (MOGA), and the niched Pareto genetic algorithm. The proposed multi-objective optimisation techniques consider the rotor radius, stator/rotor axial length, magnet thickness, and winding thickness to maximise torque while minimising volume and power loss. In ref. [126], a multi-objective design optimisation technique for AFPM brushless DC micromotors is proposed, combining response surface modelling and a unique MOMVO algorithm. With the limitations of the minimum recommended torque and the maximum required back

EMF, the optimisation's two goals were to reduce the micromotor volume and increase joule efficiency. Along with the fundamental design goals of torque and power, limiting torque ripple, reducing power loss, and reducing vibration and noise were all significant factors in the optimised design and analysis of AFPM motors for new energy vehicles. The features of the aforementioned optimisation and design techniques are compared and summarised in a table to provide an understandable overview.

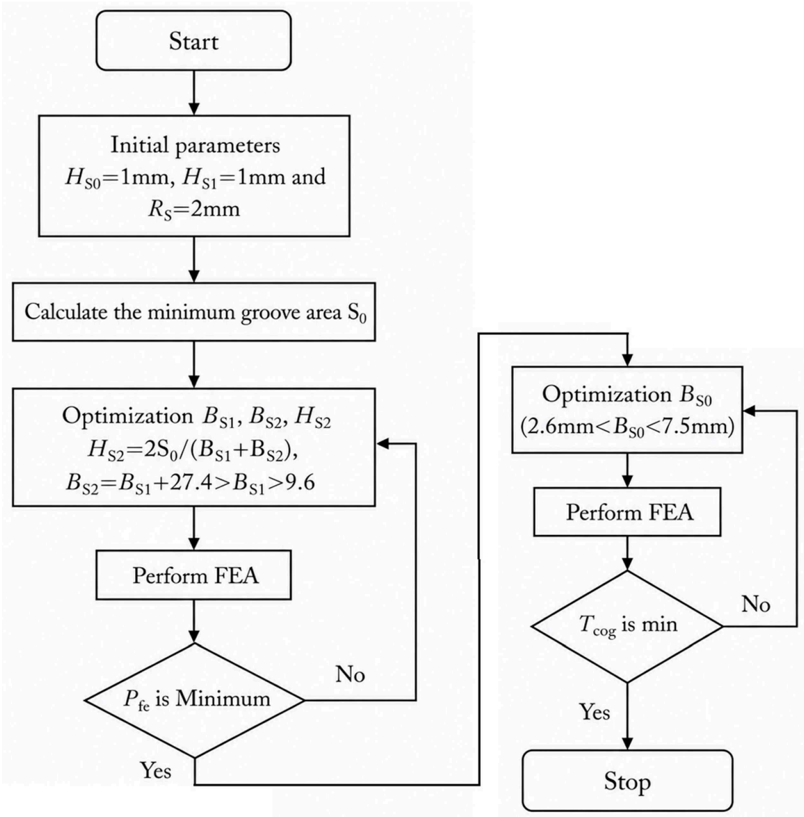

Figure 9. Example of stator optimisation procedure. Adapted from ref. [123].

As summarised in Table 3, the optimisation approaches employed for AFPM motor design can be broadly classified into evolutionary algorithms (EA). Although several optimisation techniques have been implemented in AFPM motor design, their practical applicability is highly dependent on the optimisation targets, computational resources, and desired solution fidelity. Evolutionary algorithms, in particular GA-based approaches and NSGA-II, are among the most extensively used methods due to their potential to handle highly nonlinear and contradictory objectives, such as increasing torque density while decreasing losses, cogging torque, and magnet volume. These approaches provide a variety of Pareto-optimal solutions, but they typically require a significant number of objective function evaluations, making them computationally expensive when paired with 3D-FEA.

Particle swarm optimisation achieves convergence faster and requires fewer tuning parameters than evolutionary algorithms, making it suitable for problems with medium-to-high dimensionality and limited computational budgets. However, PSO is more sensitive to premature convergence and may produce less diverse solutions in multi-objective optimisation applications. Similarly, newer algorithms, such as MOMVO and bat optimisation, have significant exploration capabilities and can produce competitive results, but their industrial validation and practical use remain limited.

Table 3. Optimisation methods with highlights.

Method (Verification)	Optimisation Targets and *Design Variables*	Strengths	Limitations	Ref.
EGA (3D-FEA)	Minimisation of permanent-magnet mass, THD, and losses; maximisation of efficiency and torque density via optimisation of *magnet dimensions, slot geometry, winding configuration, air-gap length, and current density*	Robust global search; effective for nonlinear multi-objective problems; good diversity preservation	High computational cost; slow convergence; requires tuning	[130]
NSGA-II (3D-FEA)	Multi-objective optimisation of torque ripple, electromagnetic noise, and efficiency through adjustment of *slot shape, pole arc, skew angle, winding turns, and magnet segmentation*	Produces Pareto-optimal solutions; widely validated; effective for conflicting objectives	Computationally expensive; sensitive to initialisation; long runtime	[89]
PSO (3D-FEA and experiment)	Maximisation of air-gap flux density and dynamic performance; minimisation of harmonic distortion and cogging torque via optimisation of *rotor geometry, magnet placement, slot opening, and air-gap size*	Fast convergence; simple implementation; few parameters	Risk of local minima; weaker multi-objective performance	[91]
MOMVO (against NSGA-II)	Minimisation of machine volume and losses; maximisation of efficiency and power density by optimising *core dimensions, conductor size, slot/pole combinations, and geometric scaling*	Strong exploration capability; effective for nonlinear problems	Less mature; limited industrial validation	[95]

Surrogate-assisted techniques based on artificial neural networks and response surface models have recently acquired popularity for reducing the computational burden associated with repetitive finite element simulations. By creating nonlinear correlations between design variables and machine performance characteristics, these techniques allow for rapid performance prediction while significantly reducing optimisation time. Their accuracy, however, is highly dependent on the quality and representativeness of the training data.

Overall, no single optimisation design is universally preferable. Genetic-algorithm-based approaches are often chosen when multiple competing objectives and Pareto-optimal solutions are required, although PSO-based methods are attractive for faster convergence and lower computational requirements. Surrogate-assisted optimisation is particularly useful for high-dimensional issues that require computationally intensive electromagnetic simulations. As a result, the option of an optimisation approach should be determined by the unique design objectives, available computing resources, and acceptable trade-offs between solution quality, convergence speed, and computational costs.

5.6. Materials and Manufacturing Processes

During the preparation of this review article, it was identified that one of the reasons for the lower level of commercial implementation of this type of electric motor is the complexity of manufacturing key parts of AFPM motors using traditional technologies, which results in high product prices in comparison with similar technical solutions or performance specifications. This section discusses the latest trends in AFPM motor production and materials. This section highlights the relative benefits of the popular technologies for producing windings, stators, and PM rotors reported in the literature.

5.6.1. Design and Materials of the Stator

Between AFPM motor design variations, the stator structures might differ substantially. They might be yokeless with segmented armature (YASA), coreless, or iron-cored. Laminated electrical steel is commonly used in the production of electric machine stator cores to minimise eddy-current losses. AFPM motors require radial laminations, which are more challenging to assemble than in RFPM machines, where laminations can be mounted axially. Here is a summary of several AFPM stator production techniques.

(1) PCB stator: Printed circuit board (PCB) stators are an innovative and specific type of stator winding for AFPM motors, where copper traces on a multilayer PCB replace traditional copper wire and an iron core. They are ideal for compact, high-speed applications (e.g., EVs, drones, and HVACR). PCB stators have been investigated and applied to AFPM motor design [123–126], while ref. [131] provided a detailed assessment. Tsai et al. [132] present a PCB stator with rhomboidal windings for a small spindle motor. In ref. [133], it was demonstrated that trapezoidal winding outperforms the rhomboidal pattern in terms of torque production and board area. Wave winding schemes for PCB stators were compared in ref. [134], and non-overlapping radial wave winding was identified to have the highest fundamental back-EMF and torque capability. The performances of a laminated stator and a PCB stator were compared in ref. [135]. When the output power was the same, the device with the PCB stator was more efficient and compact. Nevertheless, the PCB stator faced significant thermal limitations when attempting to achieve higher current densities. While PCB windings appear promising for low-voltage and low-current applications, they may not be suitable for higher-voltage and higher-current-density applications, given current technology levels.

(2) Soft magnetic composites: For the manufacture of AFPM stators, the use of soft magnetic composites (SMC), which are described in publications such as refs. [122,136,137], is receiving increasing attention. Compared to laminated steel, this technology may entail a higher initial cost for SMC moulds. The characteristics of SMC and laminated stator cores for a 14-pole 12-slot AFPM machine were compared in ref. [138]. It states that at lower operating speeds (lower frequency), the laminated core worked better. However, SMCs had higher efficiency than laminated cores at higher operating frequencies. This was due to increased eddy-current losses in multilayer steel. In particular, SMC can provide an isotropic three-dimensional magnetic flux, reducing losses by 20–50% at high frequencies (>1 kHz) compared to laminated plates, thanks to its isolated iron particles (10–100 microns). SMC obtained by pressing into a given shape simplifies designs with YASA, reducing iron weight by up to 80% and noise and vibration levels by eliminating magnetostriction [139].

(3) Laminated steel: Toroidal slotless AFPM stators, such as those shown in refs. [140–142], have been produced by using tape-wound cores constructed from thin-gauge electrical steel. This is a common, reasonably uncomplicated method that is not required for specific production equipment or processes. Slotted-stator AFPM motor variations can be constructed by creating slots in the tape-wound cores. Sahin [143] formed slots in a tapewound core for a 30 kW, 16,000 RPM axial-flux generator using the wire electrical discharge machining (EDM) technique. In ref. [144], a similar strategy was used, but the slots were machined rather than cut. It was observed that short circuits between the lamination layers could be introduced during slotting machining. Conventional AFPM motors employ laminated silicon steel (e.g., M19–M36 grades) for stators and rotors, offering low core losses at low frequencies (<400 Hz) via radial punching or spiral winding. However, complex geometries increase manufacturing costs and eddy currents at high speeds (>3000 rpm). Therefore, new materials and production solutions are currently being developed.

(4) Additive manufacturing: Additive manufacturing (AM), particularly laser powder bed fusion (LPBF) or binder jetting of Fe-Si or Fe-Co powders, fabricates intricate cores with

tailored microstructures. These techniques are currently being investigated for AFPMs e.g., Refs. [145,146]. Sun et al. [122] compared laminated, SMC, and additively manufactured stators in a multi-stage AFPM motor test. The additively manufactured stator has lower core losses than laminated and SMC stators at both low and high frequencies (above 1 kHz). In addition to the stator core, windings for additive manufacturing can be produced using various techniques.

Moreover, stator design can reduce cogging torque by optimising slot openings, tooth pairing, teeth notching, displacement, skewing of stator teeth, dummy slots, filling slot openings, and displacement of dual stators [147]. Letelier et al. [148] studied how to reduce cogging torque in a single-stator dual-rotor AFPM motor using stator-slot displacement and skewing. Combining stator-slot displacement with skewed-rotor PM can reduce cogging torque by up to 60%. Wanjiku et al. [147] investigated the effect of stator-slot dimensions and tooth profiles on the cogging torque of AFPM motors. Four alternative tooth shapes were tested to demonstrate that implementing a parallel tooth profile with a trapezoidal slot profile reduced cogging torque by 24% without modifying the rotor construction. The evaluation of several strategies to reduce cogging torque in AFPM motors in ref. [149] demonstrated that shifting the slots and slot openings can decrease cogging torque. It was demonstrated that a 1/2-slot-pitch displacement of the stator-slot openings can reduce the cogging torque by about 25%. Skewing stator slots can minimise cogging torque, but it also increases leakage inductance and copper loss due to increased winding length [148]. In addition, depending on the manufacturing technique used, creating stators with skewed slots can be problematic.

In summary, the cost, efficiency, and compactness of AFPM machines are significantly impacted by the selection of stator materials and manufacturing methods. While SMC materials and additive manufacturing offer benefits for high-frequency operation and complex shapes, laminated steel remains the optimal conventional solution. Compact and effective low-power designs are made possible by PCB stators, although they are constrained by thermal issues. Overall, ongoing advances in materials science and manufacturing processes are expected to improve the performance, scalability, and economic viability of AFPM machines.

5.6.2. Design and Materials of Rotor

Non-standard PM shapes are typically required for AFPM rotors, and they can be expensive to produce. High-performance rotors using conventional-shaped PMs have been modified in the literature to reduce costs (e.g., Refs. [150–152]), and they use smaller PM segments per pole, which are considered cost-effective and help to reduce induced eddy-current losses. Vansompel et al. [150] analysed a 4 kW, 2500 RPM YASA machine with a T-shaped pole configuration and various magnet segment numbers. This final pole structure comprises 14 cuboidal NdFeB segments per pole, resulting in an 8x reduction in eddy-current losses compared to unsegmented poles.

Reports on Halbach arrays rotors for AFPM motors can be found in various research studies [153–155]. Because of their intrinsic sinusoidal air-gap field distribution and flux-focusing capacity, these rotors are commonly employed in ironless-stator AFPM machines. A comprehensive mechanical design of a Halbach array rotor for a 50 kW coreless AFPM motor was published by Zhang et al. [154]. The prototype demonstrated mechanical stability while reaching up to 9000 RPM. In comparison to an axially magnetised PM array, a quasi-Halbach array rotor was found to improve a torus machine's torque density by 12% [153].

Additionally, PM forms can be applied as a design handle to enhance machine performance. In refs. [156–158], the impact of PM shape on AFPM motor performance was investigated. To minimise the cogging torque of double-rotor AFPM machines, various commercial PM forms and skewing methods, depicted in Figure 10, have been investigated and evaluated.

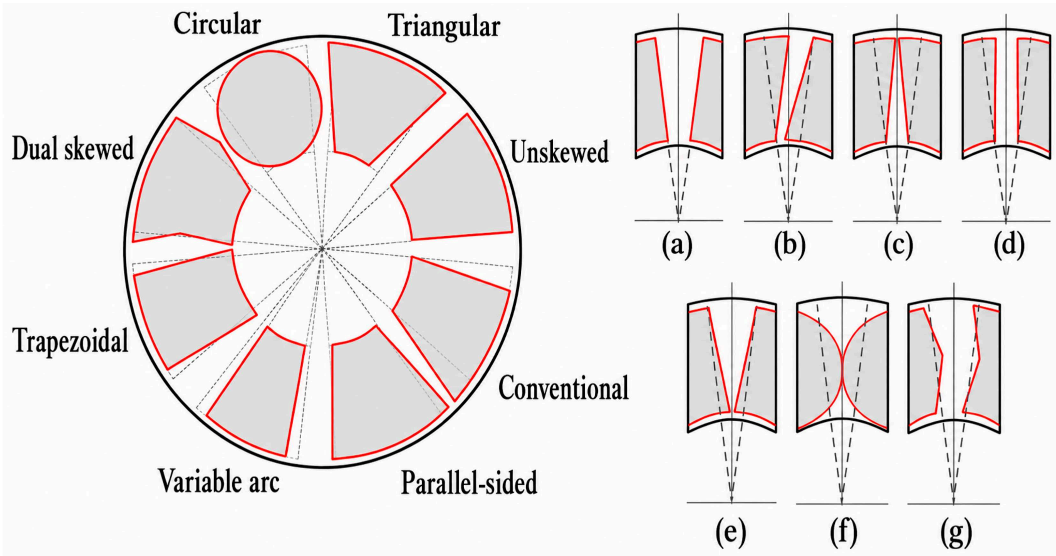

Figure 10. Rotor disk PM forms and skewing techniques for AFPM motors: (**a**) unskewed, (**b**) conventional, (**c**) triangular, (**d**) parallel-sided, (**e**) trapezoidal, (**f**) circular, and (**g**) dual-skewed.

Different stator tooth and slot geometries are used in AFPM machines to improve electromagnetic performance and reduce cogging torque. Circular and curved profiles offer improved magnetic-flux distribution and reduced stress concentration, but they are more difficult to produce. Triangular and trapezoidal shapes minimise cogging torque and enhance flux shaping, but they may also increase local magnetic saturation and manufacturing complexity. Conventional and parallel-sided slot designs remain common due to their simple construction, ease of winding placement, and low production costs; however, they often exhibit higher torque ripple than optimised geometries. Unskewed stators offer high torque density and ease of production, but they often generate greater cogging torque and vibration. Dual-skewed and inclined slot layouts minimise cogging torque and acoustic noise but increase winding length, copper losses, and production complexity. Overall, optimised irregular or variable-arc geometries can deliver optimal electromagnetic performance, but this typically comes at the cost of more complex production techniques.

Regarding the unskewed design, the triangular skew was found to significantly reduce cogging torque and achieve performance comparable to the traditional skew. For a coreless AFPM motor, an interior permanent-magnet (IPM) rotor design with sinusoidally curved magnets was suggested in ref. [157]. Compared to a standard conventional coreless AFPM, this design had 60% lower THD and was 35% more torque-dense. Wanjiku et al. [147] tested the following PM configurations to lower the cogging torque: (i) a pole-arc ratio of 0.81, (ii) alternating pole-arc ratios of 0.61 and 0.81, and (iii) skewed by one pole pitch. Switching pole arcs successfully reduced cogging torque by 73% when compared to a 0.81 pole-arc rotor, although skewed poles reduced cogging torque by 48%.

Using 3D FEA, Aydin et al. [149] evaluated the effectiveness of several cogging-torque-minimisation strategies for AFPM machines and showed that skewing the rotor PM or the stator slots effectively reduced cogging torque. It was demonstrated that adding an 18.75 degree magnet skew decreased the peak-to-peak cogging torque of a p = 4-pole-pair machine from 16 Nm to about 3 Nm. Techniques such as triangular skew, trapezoidal skew, parallel magnets, circular skew, and dual-skewed magnets were assessed in addition to traditional skewing. According to the findings, the circular and triangular skews provided cogging torque reductions of roughly 77.5% and 84.3%, respectively, with comparatively small additional expenses for the unique PM forms.

Ali et al. [159] investigated curved PM and curved PM with skew, demonstrating that they achieved approximately 40% and 44% reductions in cogging torque, respectively, compared to skewed PM with a conventional flat PM face profile. Further novel PM geometries, such as curved and elliptical PM face profiles, were also investigated in ref. [160] to reduce cogging torque in AFPM motors. The authors suggested an elliptical face profile and contrasted it with the curved and flat PM face profiles to demonstrate that, compared with the traditional flat PM face profile, the elliptical profile offered a roughly 17% reduction in cogging torque.

In AFPM electric machines, the windings are usually placed on a toroidal magnetic core and form a three-phase system consisting of concentrated or distributed coils. The conductors are laid in the radial slots of the toroidal core or arranged in a slotless configuration directly in the air-gap zone. In this case, the active parts of the coils are oriented radially, while the end parts are oriented axially, resulting in shorter end parts and lower hysteretic losses than in FPM machines [161].

The conductor material is almost always high-purity electrolytic copper (Cu-ETP or Cu-OF) due to its high electrical conductivity (≈58 MS/m) and good thermal characteristics. Highly efficient AFPM machines widely use conductors with rectangular or square cross-sections, as this geometry provides a higher slot fill factor, reduces air gaps between turns, and improves heat transfer to the magnetic circuit. For example, the experimental machine described by Caricchi et al. [162] used a rectangular copper wire measuring 5 mm × 1.12 mm, placed in slots 12 mm deep, enabling the formation of compact coils with low resistance and high current density.

The requirements for efficiency, frequency, and thermal conditions of the motor determine the wire shape and winding structure. The following types of conductors are most common:

- Round wire—Used in small and medium-sized machines due to its ease of winding, but it has a lower fill factor.
- Rectangular or profile wire—Provides denser packing, reduced resistance, and improved thermal contact; widely used in traction AFPM motors.
- Litz wire (multi-strand insulated wire)—Used in high-frequency machines to reduce losses from skin effect and eddy currents.
- Pre-formed coils—Used in high-power machines to improve reproducibility and fill factor.

Aluminium may also be used as a winding conductor in AFPM machines, especially in applications where weight and cost are critical. Due to its lower electrical conductivity compared to copper, a larger conductor cross-section is generally required to achieve comparable resistance. Nevertheless, aluminium offers a significant advantage in mass reduction due to its much lower density. This makes it particularly attractive for lightweight systems such as robotic and aerospace drives. Certain challenges, including oxide formation and lower mechanical robustness, must be addressed through appropriate design and manufacturing techniques. Recent work has demonstrated the use of anodised aluminium foil windings in axial-flux machines, showing promising results in terms of reduced weight, good thermal performance, and suitability for compact direct-drive robotic actuators [163].

Therefore, optimising the material, conductor shape (rectangular profile), and winding topology (concentrated or distributed) is critical to achieving high power density, efficiency, and thermal stability in axial-flux permanent-magnet electric machines.

To complement the advantages and limitations discussed above, these four routes differ markedly in industrial maturity. SMC cores are the closest to industrial maturity, as they are commercially produced and used in series motors—their main constraints being the press-tonnage limits on large cores and the reduced saturation polarisation that restricts high-torque designs. PCB stators have also reached the market, although only in compact, low-power, and high-speed machines. They inherit the repeatability and low unit cost of conventional board manufacturing, but the thin conductors and modest thermal headroom keep them far from traction power ratings. Aluminium windings rely on a mature, low-cost, and lightweight material, yet their use in AFPM stators remains largely at the prototype stage owing to higher resistivity and joining difficulties that erode efficiency. Additive manufacturing is the least mature, remaining at the laboratory-validation level. It is attractive for integrated cooling and topology-optimised parts but is still constrained by throughput, build volume, and cost, which prevent volume traction production. Overall, for near-term readiness and scalability in high-power traction, the technologies rank approximately as SMC > PCB stators > aluminium windings > additive manufacturing. Taken together, only SMC and, in their niche, PCB stators can presently be regarded as production-ready, whereas aluminium windings and additive manufacturing are better viewed as promising routes that still require development before they suit high-power traction.

5.7. Thermal Management

Higher current density and electric loading are only possible with efficient thermal management, which can increase the overall power density of electric machines [81]. Additionally, it may reduce the likelihood that the rotor PM will thermally demagnetise. Since AFPM motors typically implement torque-dense and power-dense designs, temperature control is also a crucial design factor for these machines. This section reviews the thermal management strategies applied to AFPM. Most of these methods focus on cooling the stator windings, whereas there is little research on rotor cooling methods.

Numerous methods for cooling AFPM stators have been described in the literature, including refs. [164–167]. In turn, ref. [168] provides an in-depth evaluation of AFPM motor thermal-control strategies. Lindh et al. [165] directly cooled the stator windings of a dual-stator single-rotor AFPM motor using a specially adapted Litz wire. It was demonstrated that replacing the coolant-carrying tube in the core of the conductor bunch increased the continuous current density by a factor of 3.5. Rahman et al. [169] cooled the stator end windings of a toroidally wound AFPM motor by wrapping the stator windings with an aluminium jacket, as seen in Figure 11a. Direct oil cooling of the end windings, as suggested in ref. [170] and illustrated in Figure 11b (above the oil flows, of course, an aluminium jacket is also assumed). According to the results reported in ref. [170], direct oil cooling can achieve stator-winding current densities approximately twice those obtained with conventional water-jacket cooling.

There have also been reports of methods for cooling AFPM motor rotors, such as in refs. [171,172], which proposed a combination of forced air and a hollow rotor shaft with water channels and compared it with stator water-jacket cooling and forced-air cooling. Coolant flowing through the hollow rotor shaft may affect rotor dynamics and pose an issue at high speeds, despite the method's ability to efficiently cool the rotor.

In ref. [173], the thermal management demands of AFPM and RFPM motors were compared at various aspect ratios (the ratio of outer diameter to axial length). Analysing the different aspect ratios of AFPM and RFPM motors revealed that, on average, the AFPM motor requires less cooling than the equivalent RFPM motor. For the specified application and machine ratings, the AFPM motor achieved a temperature rise that was about 26% lower at an aspect ratio of 0.38. These analytical findings were confirmed by experimental data from a prototype coreless AFPM motor. These results indicate that, in comparison to similar RFPM motors, AFPM motors have comparatively lower thermal management requirements.

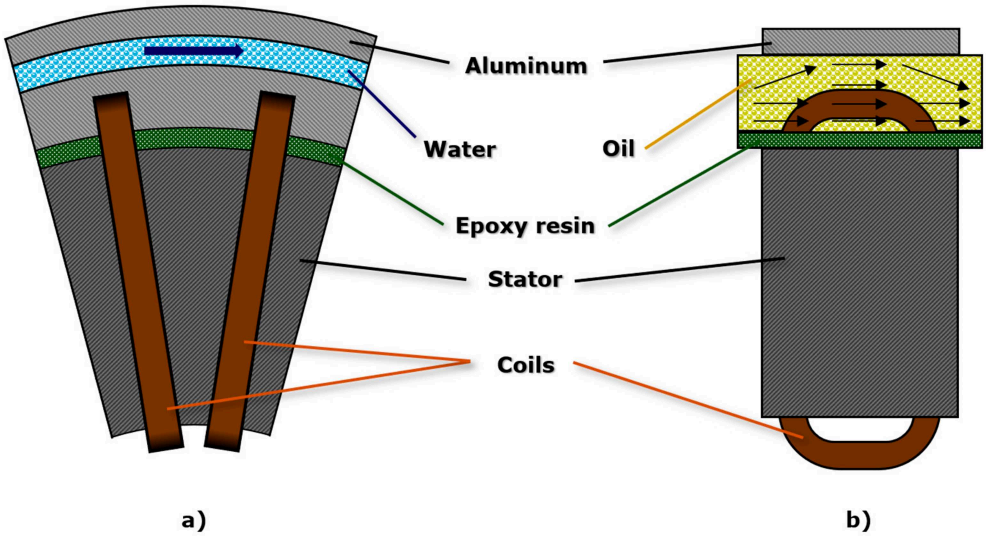

Figure 11. Cooling techniques for stator end windings of torus machines: (**a**) water and aluminium jacket; (**b**) direct oil cooling (the jacket is also supposed above the coils). Adapted and modified from ref. [170].

Another example of oil-cooling system architecture for an AFPM machine by Traxial BV illustrates the circulation of lubricant through the machine and its auxiliary components (Figure 12). Configurations of this type typically combine pumps, filters, a heat exchanger, and an external reservoir, which are commonly considered in direct oil-cooling applications. Since the arrangement and dimensions of individual components depend strongly on the machine topology, thermal requirements, and available installation space, the scheme is intended only to demonstrate one possible layout rather than a specific industrial design. A similar concept was examined during the initial stages of the CliMAFlux project; however, the final solution was substantially adapted to satisfy project-specific requirements and is therefore not publicly available. Consequently, the configuration shown in Figure 12 should be viewed as a generic example of an oil-cooling and lubrication circuit and not as the final implementation integrated in the project.

The closed-loop oil circuit consists of a scavenger pump, an oil feeding gear pump, a reservoir, a heat exchanger, and a multi-stage filtration system. Oil is supplied to the machine through the inlet channel to provide direct cooling and lubrication of critical motor components, and it is collected through the outlet and dry sump sections. Temperature (T), flow (F), and pressure (P) sensors are integrated throughout the system for real-time condition monitoring. Additional rotor and stator outlet filters, together with a fine membrane filter (10 μm, $\beta > 75$), ensure oil cleanliness and operational reliability. The heat exchanger regulates oil temperature to maintain optimal thermal performance of the AFPMSM. In brief, thermal management remains one of the most challenging design concerns for AFPM machines due to their high torque and power density. Existing research indicates that effective cooling solutions, particularly direct-winding cooling and oil-based thermal management systems, can significantly increase acceptable current density while improving operational reliability. While most research has focused on stator cooling, rotor-cooling methods are also being explored, especially for high-speed applications. Comparative studies also show that AFPM machines may have lower thermal management needs than identical RFPM machines under certain operating situations. Overall, efficient cooling is critical to ensure stable thermal behaviour, minimise PM demagnetisation, and realise the high-performance potential of AFPMS.

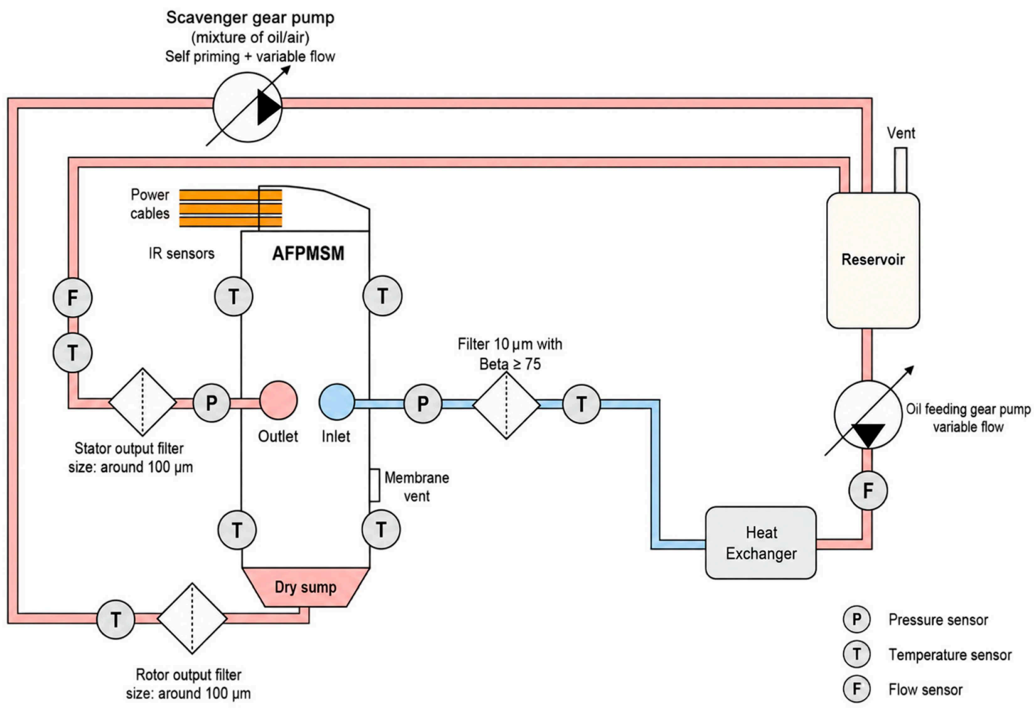

Figure 12. Schematic representation of the oil-cooling and lubrication circuit for the AFPM motor by Traxial BV.

6. Control Strategies

Axial-flux permanent-magnet motors are widely used in modern industrial and transportation applications that demand outstanding performance, high precision, and reliable operation. Their compact structure, high torque density, and superior efficiency make them particularly attractive for advanced drive systems. By contrast, torque linearisation in separately excited DC machines is relatively straightforward because torque and magnetic flux can be controlled independently, allowing for simpler control strategies. However, despite the inherent nonlinear characteristics of AFPM motors—arising from magnetic saturation, coupling effects, and parameter variations—they are increasingly preferred over DC motors in medium- and high-power drive applications due to their higher efficiency, reduced maintenance requirements, and improved dynamic performance. Various control techniques have been developed to linearise and decouple AFPM motors. They typically use several control approaches, including field-oriented control (FOC), direct torque control (DTC), model predictive control (MPC), and others. All of the techniques listed above are discussed in the current section of this review.

6.1. Field-Oriented Control

Among traditional control systems, FOC or vector control is frequently used to regulate the AFPM motor. FOC requires the use of a frequency converter to regulate the excitation and torque currents autonomously [174]. Tsai et al. [132] proposed a vector-control technique for an AFPM motor powered by a current source inverter (CSI), which offers several advantages over voltage-source inverters. The control system provides precise control and rapid dynamic reaction thanks to its 2-DOF speed controller, multi-loop current controller, and space-vector pulse-width modulation (SVPWM).

Wilson et al. [175] evaluated the performance characteristics of a double-rotor–axial-flux PMSM for in-wheel EV applications using a sensorless optimal vector-control approach. The performance research was carried out using a sensorless vector-control technique based on a higher-order sliding mode observer (SMO) with a super-twisting algorithm. Because mechanical sensors were no longer required, the system was smaller and less expensive, which is beneficial for EVs. A particle swarm optimisation technique was applied to optimise the proportional-integral speed controller gains in the vector-control scheme, thereby minimising speed and torque ripples. The novel hybrid-excited motor, termed the hybrid axial-field flux-switching permanent-magnet machine (HAFFSPMM), combines the benefits of axial-field flux-switching and hybrid-excited synchronous machines.

Zhao et al. [176] investigated the HAFFSPM machine's performance over the entire working range and suggested mathematical modelling of the device using vector control. The performance of traditional PI-based FOC in drive systems deteriorates due to parameter changes caused by ageing and increased temperature. Akhil et al. examined the performance of an LUT-based FOC with SMC for EV drivers [177]. A sensorless AFPM motor-control technique is presented in ref. [178] for in-wheel EV applications. Starting and rotor-position rotation estimates are part of the sensorless control strategy for the proposed flux-modulation motor. An SMO is applied to estimate the rotational position, and a rectangular-pulse-voltage injection is used to estimate the starting rotor position, providing a new online self-adjustment technique for the SMO that addresses saturation effects on inductances caused by rectangular-pulse voltage injection. This impact reduces the SMO's precision and alters stator characteristics under different loads (see Figure 13).

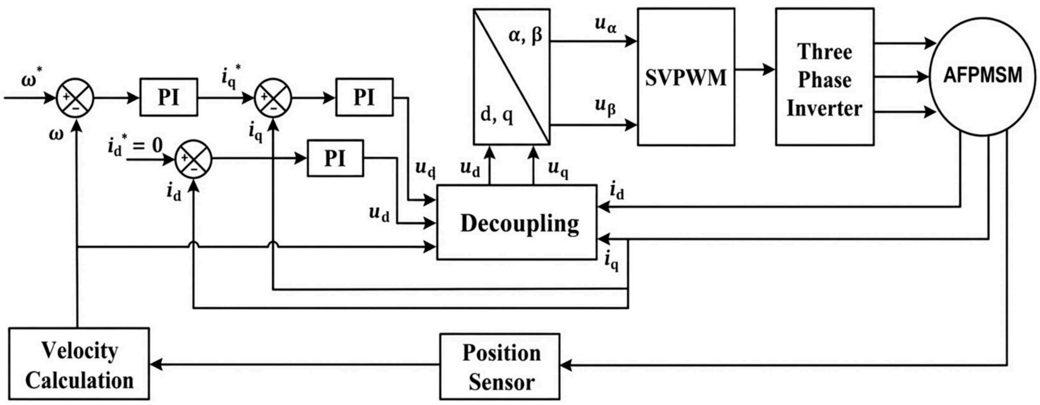

Figure 13. Adapted block diagram of vector control for AFPM machines [179].

Liu et al. [180] developed an accurate evaluation technique to maximise the torque performance of a single-sided permanent-magnet axial-flux motor (SPMAM), which successfully identified the optimal operational torque trajectory. The study concluded that ideal conditions can be achieved by appropriately adjusting the current shifting angle. SPMAM's propulsive and axial forces were analysed within the operating limits to meet mechanical design criteria and maximise application benefits. The SPMAM provides full operational control via the current-shifting angle, and its linear torque control and axial force reduction capabilities improve overall performance in applications such as EVs when used with the appropriate controller.

6.2. Direct Torque Control

Among the many different motor-control strategies, direct torque control is a significant one. By selecting the correct voltage vector, it independently controls the torque and flux linkage [181]. The fundamental idea of DTC is to calculate the instantaneous flux and torque from the stator machine variables, then apply a preset switching table to select a suitable voltage vector. DTC enables direct, independent control of these parameters by selecting optimal inverter-switching states and limiting flux and torque errors with hysteresis controllers [182]. By measuring and computing the shaft torque and magnetic-flux linkage vector, comparing the results with reference points, and making successive adjustments to maintain the intended performance, DTC regulates shaft torque. Malyshev et al. [183] presented a DTC algorithm for the AFPM motor, and their findings showed a notable reduction in torque and stator magnetic-flux vibrations compared to the basic FOC. The model's output showed little torque ripple and good dynamic and steady-state performance. This technique had sufficient control settings, resulting in a short rising time (0.049 s), an acceptable steady-state error (0.23%), and little overshoot (0.1%) [70] (see Figure 14).

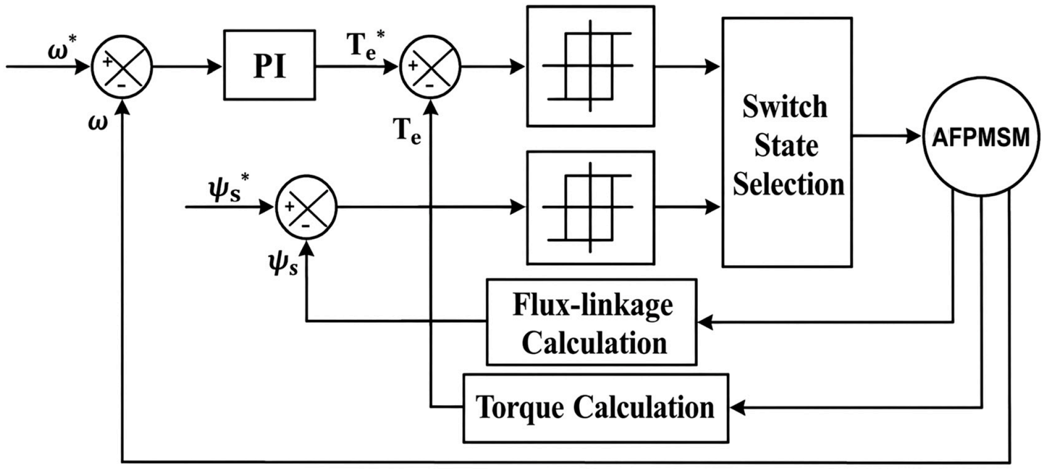

Figure 14. Adapted block diagram of direct torque control for AFPM machines [179].

Fard et al. proposed a twisted model that outperformed traditional AFPM machines in efficiency and back-EMF, with the controller serving only as a speed loop, with no current or hysteresis control, thereby improving the AFPM motor's dynamic performance. A new yokeless, segmented, axial-flux, flux-switching, sandwiched-permanent-magnet (YASA-AFFSSPM) motor for in-wheel drive applications was proposed to enhance torque and winding area [117]. Sensorless control drives were used to analyse the static and dynamic performance of the YASA-AFFSSPM, resulting in lower cogging torque and higher torque density [184]. An algorithm for sensorless direct torque control of AFPM motors using back-EMF was presented by Anisi et al. [185]. Without requiring a powerful processor, it was able to estimate the rotor location and speed and function well even at low speeds. This approach provides effective control over a wide speed range, making it ideal for hybrid EVs. Although it depends on the motor's internal settings and creates higher torque ripple, it allows direct wheel control, compact electronic components, and an immediate torque response.

6.3. Improved FOC and DTC

To improve control performance, some studies have proposed modified FOC and DTC systems to address their shortcomings. For example, in ref. [186], a sliding-mode vector-control system for EVs based on cooperative optimisation of AFPMSMs was proposed. The torque-tracking capability, speed-limiter features, and operating characteristics of EVs could all be enhanced by the proposed sliding-mode vector-control method. Yang et al. [187] proposed a novel vector control based on three magnetisation state (MS) manipulations for axial-field flux-switching memory machines (AFFSMMs) to address excitation copper loss and a limited speed range. The modified FOC control algorithm reduced speed and torque overshoot and improved the dynamic performance of AFFSMMs compared with the PI technique. Based on the efficiency-optimal torque-distribution approach, Zhao et al. [22] developed a deadbeat current-predictive vector-control system using the three-stator double-rotor AFPMSM as the study object. The torque-tracking characteristics were significantly improved by the suggested deadbeat current-predictive vector-control method, which also achieved minimal torque ripple and no torque overshoot in the steady state. Furthermore, to improve the control performance and accuracy of AFPM motors, some studies have proposed control strategies based on sliding observers [16,175] and extended disturbance observers [188,189].

An adaptive sliding mode observer (ASMO)-based improved control strategy was developed by Zhai et al. [190]. This method uses a phase-locked loop (PLL) combined with an improved ASMO to generate an extended electromotive force, enabling accurate monitoring of the rotor-pole position. The second-order generalised integrator (SOGI) is integrated into the PLL to improve position estimation accuracy, reduce vibration, and enhance system robustness. The updated ASMO with SOGI improves the machine's effectiveness and accuracy.

The performance of AFPMSMs is affected by unexpected ripples in the electromagnetic torque. Farhan et al. [191] proposed an intelligent control technique to improve the dynamic performance of AFPM motors and minimise torque ripple. The technique enhances speed and torque regulation by utilising FOC and decoupling. Using PI-PSO data for training, the adaptive neuro-fuzzy inference system (ANFIS) was implemented to continuously manage torque and speed limitations. This method significantly improved speed performance in several scenarios. A speed-constrained and current-vector-control strategy employing SMC was proposed and investigated to improve torque-tracking precision, speed limits, and overall operational performance [186]. Tests of endurance and acceleration indicated that this control approach substantially improved the cruising range and accelerating capability of EVs. Building on the average torque distribution strategy, Zhao et al. [22] presented an optimum torque distribution method to increase the range of high efficiency. A backpropagation (BP) neural network was used to find an efficient torque distribution. A current-control strategy based on deadbeat current prediction was also introduced to improve torque-tracking performance (see Figure 15).

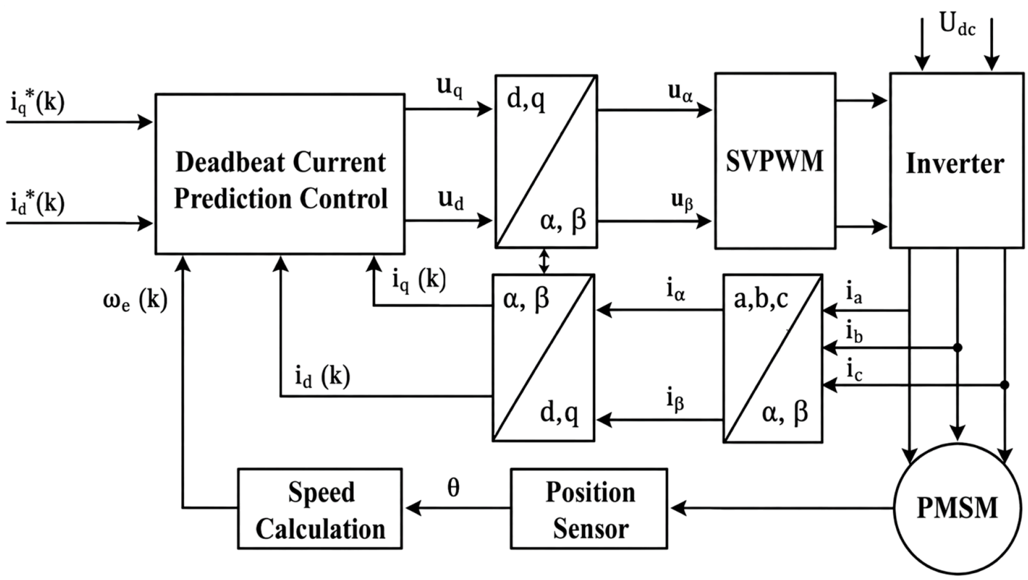

Figure 15. Adapted schematic diagram of deadbeat predication control for PMSMs [22].

6.4. Novel Control Strategies

MPC [192] and adaptive robust control (ARC) [193] are unique control strategies proposed by several researchers to improve the dynamic response performance of AFPM motors, driven by advances in control and optimisation theory. A continuous-control-set MPC (CCS-MPC) technique was introduced in ref. [176] for an AFSFPM machine to evaluate its operational performance throughout the entire speed range. The control technique combined a maximum torque per ampere (MTPA) in the constant torque area with a maximum output power flux-weakening method in the constant power region. Additionally, the MPC technique enhanced the system's resistance to load disturbances and improved dynamic performance (see Figure 16). Given its ease of implementation, quick dynamic response, and excellent tracking precision, MPC is widely used in vehicles and the control industry [25].

Another variation of predictive control, known as model predictive torque control (MPTC), has also been applied to AFPM machines. An MPTC approach for a 13-pole, 6-slot AFFSPM motor was proposed by Yuan et al. [179] after evaluating the motor's topological structure. The reference flux-linkage amplitude was set to a fixed value, ψ_s, and the torque reference value was collected via the speed outer loop's PI controller. The suggested MPTC approach achieved the least torque ripple and the fastest torque response speed compared to VC and DTC. Additionally, the flux-linkage ripple of the MPTC was only around 1.5%, which was significantly smaller than the 15.3% flux-linkage ripple under DTC.

To further enhance the performance of predictive torque control, an improved strategy, MPTC with duty-cycle control (MPTC-DCC), was developed. This approach optimises the duration of the active voltage vector to minimise torque and flux ripples, thereby improving the drive system's steady-state characteristics. The MPTC-DCC method demonstrates superior performance compared with the conventional MPTC approach, particularly in terms of ripple suppression. In addition, the integrated flux-adjustment strategy enhances the load capacity across the entire speed range and effectively extends the constant-power operating region.

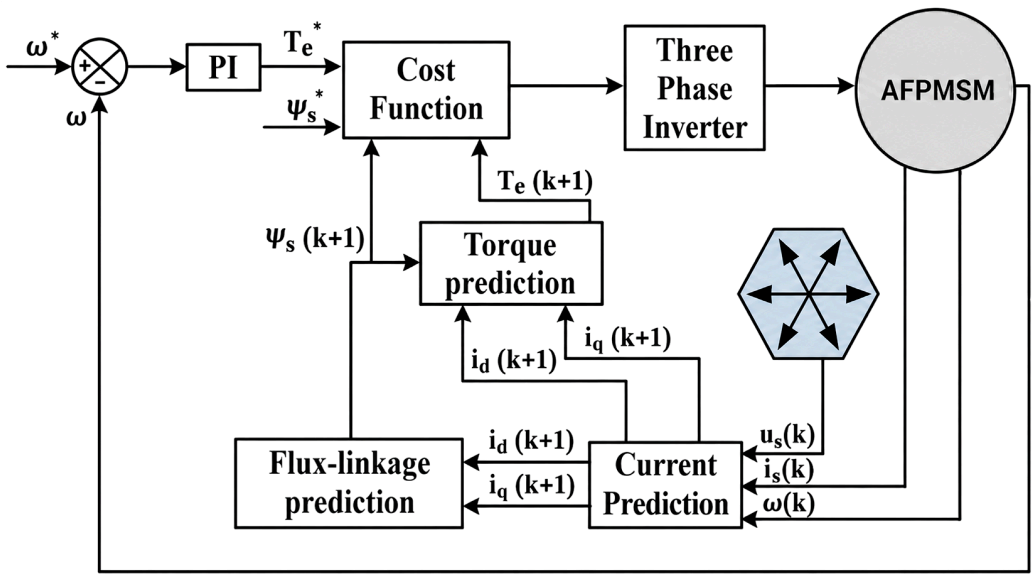

Figure 16. Adapted block diagram of MPC method for AFPMSMs [179].

The adaptive robust control (ARC) approach can modify the controller's structure and continuously collect the input, state, output, and performance parameters of the controlled system [187,194]. As a result, ARC can achieve the best control performance while maintaining the system's robustness. With a focus on anti-disturbance control, Wang et al. [78]

investigated and suggested an adaptive robust drive control system for an AFPMSM of an electric medium-sized bus based on the optimal torque distribution approach. Zhang et al. [195] investigated sensorless control methods based on the model reference adaptive system (MRAS) for a hybrid excitation axial-field flux-switching permanent-magnet machine (HEAFFSPMM). Simulation and experimental results demonstrated that the proposed ARC method enhanced the drive system's control accuracy and effectively suppressed disturbances. Three speed-sensorless control algorithms—stator currents, stator flux links, and simplified stator currents—were included in the MRAS observer for speed, which was implemented using the FOC technique. The MRAS method, based on simplified stator-current measurements, demonstrated high control accuracy and good performance, as evidenced by simulation and testing results.

7. Discussion and Conclusions

This review article brings together and analyses key aspects of AFPM motors. The focus of the research was on recent advances in topologies, design optimisation methods, materials and manufacturing, and control techniques for these complex devices. In general, this type of PMSM has enormous potential for use in ground vehicles due to its high-power density and the potential to minimise cogging torque. Among the various topologies, the YASA and AFIR variants are the most popular according to the literature reviewed. In addition, modern developments place considerable emphasis on the materials used. For example, AFPM motors with printed circuit board (PCB) windings can provide improved electromagnetic performance through optimised winding layouts, although the increased effective air-gap length generally results in a lower air-gap flux density. The use of aluminium windings also shows promising results in optimising production and the technological process. Of course, in the future, it is necessary to continue simplifying the design and exploring the use of more affordable materials, both in terms of price and supply chain. For design and optimisation, the starting point is determining the diameter ratio. Subsequent specification indicators, such as power loss, torque ripple, and vibration noise, are also important considerations in the design of AFPM motors. Existing design optimisation methods, including genetic algorithms, particle swarm optimisation, and artificial neural networks, have proven their effectiveness in certain scenarios and have demonstrated efficiency gains of up to 15% under realistic driving cycles. As for simulation methods and models, an optimised method is being developed in this area. It includes the ability to transform the three-dimensional model of AFPM motors into a quasi-three-dimensional model by leveraging FEA and MEC analyses. Based on this, it is possible to integrate multi-objective optimisation-design theories into AFPM optimisation, enabling maximum modelling accuracy and effective analysis with moderate computational requirements. Multi-objective frameworks have also effectively balanced torque ripple, magnet cost, and core saturation.

The control techniques discussed in this review place high demands on the control system as a whole, particularly in terms of stability, reliability, and computational simplicity. Strategies such as MPC, sliding mode control (SMC), and sensorless vector control have been reported to enhance dynamic performance and to reduce the harmonic distortion of the output torque compared with classical methods such as FOC and DTC. The magnitude of these improvements, however, is strongly case-dependent, varying with machine topology, power and speed range, and operating conditions, so the values reported in individual studies should be regarded as specific to those conditions rather than as general figures for AFPM drives. It is expected that control strategies for AFPM motors will be further investigated and refined in the future, with a focus on intelligence level, dynamic response, and robust performance.

This study suggests important research paths in multiphysics modelling, adaptive control techniques, and cost-effective manufacturing processes, benchmarking these areas against technological limitations today. The findings provide an in-depth basis for the development of next-generation PMSM systems with improved fault tolerance, compactness, and high efficiency.

Based on the conclusions discussed above, it is expected that new topologies, precise optimisation processes, material analysis, and advanced control strategies will contribute to the continuous improvement of AFPM motor performance. Therefore, to meet the high demands of modern EVs, future research will focus on optimising motor design, including reducing manufacturing costs and end-product prices, as well as improving the dynamic characteristics of AFPM motors.

Research Gaps and Future Directions

Even though there have been significant advancements in recent years, there are still a number of important issues that prevent AFPM technology from being effectively used. The following research topics should receive special attention in this context:

1. Multiphysics modelling and thermal management.
   This represents the most immediate challenge for AFPM machines. As these motors are increasingly used in high-power-density applications, such as electric vehicles, aerospace systems, and marine propulsion, electromagnetic, thermal, mechanical, and fluid-dynamic phenomena become strongly coupled. Accurate multiphysics models are therefore essential for predicting machine behaviour, improving reliability, and avoiding excessive temperatures and irreversible demagnetisation.
2. Materials and manufacturing technologies.
   The cost and availability of rare-earth magnets, together with the demand for lightweight and sustainable solutions, remain major barriers to the widespread adoption of AFPM machines. Consequently, further research on soft magnetic composites, reduced rare-earth magnet compositions, aluminium windings, PCB technologies, and additive manufacturing is particularly important for improving cost-effectiveness and enabling large-scale industrial deployment.
3. Control strategies and fault tolerance.
   Although considerable progress has been achieved in sensorless control and intelligent diagnostic techniques, fault-tolerant operation remains insufficiently developed. This issue is particularly important for safety-critical applications, including aerospace, marine propulsion, and high-reliability electric drives, where continuous operation and robustness are essential.
4. Digital engineering and X-in-the-Loop architecture.
   The development of model-, software-, and hardware-in-the-loop methodologies, together with digital twin technologies, is expected to accelerate the design process and improve system validation. These approaches can also support predictive maintenance and reduce development time. However, compared with thermal management and material optimisation, their industrial implementation can be regarded as a medium- to long-term objective.

Overall, multiphysics modelling and thermal management currently represent the highest priority, as they directly limit the achievable power density and reliability of AFPM machines. Material innovations are essential for improving economic competitiveness, whereas advanced control strategies and digital validation environments are expected to support the next generation of highly reliable and intelligent electric drive systems.

Author Contributions: Conceptualization, R.T., M.G., V.S., M.D. and V.I.; methodology, R.T., M.G. and V.S.; software, R.T.; validation, R.T. and V.S.; formal analysis, R.T. and M.G.; investigation, R.T. and V.S.; resources, R.T., M.G., V.S., M.D. and V.I.; data curation, R.T.; writing—original draft preparation, R.T., M.G. and V.S.; writing—review and editing, R.T., M.G., V.S., M.D. and V.I.; visualization, R.T.; supervision, M.D. and V.I.; project administration, M.D. and V.I.; funding acquisition, M.D. and V.I. All authors have read and agreed to the published version of the manuscript.

Funding: This study was funded by the European Union within the project CliMAFlux Horizon Europe (Grant agreement ID: 101096062 https://climaflux.eu/ (accessed on 4 July 2026)). The views and opinions expressed are, however, those of the author(s) only and do not necessarily reflect those of the European Union or the European Climate, Infrastructure and Environment Executive Agency (CINEA). Neither the European Union nor the granting authority can be held responsible for them.

Institutional Review Board Statement: Not applicable.

Informed Consent Statement: Not applicable.

Data Availability Statement: No new data were created or analyzed in this study. Data sharing is not applicable to this article.

Conflicts of Interest: The authors declare no conflicts of interest. The funders had no role in the design of the study; in the collection, analyses, or interpretation of data; in the writing of the manuscript; or in the decision to publish the results.

Abbreviations

The following abbreviations are used in this manuscript:

Abbreviation	Definition
AFPM	Axial-Flux Permanent Magnet
AFPMSM	Axial-Flux Permanent-Magnet Synchronous Motor
RFPM	Radial-Flux Permanent Magnet
RFPMSM	Radial-Flux Permanent-Magnet Synchronous Motor
PM	Permanent Magnet
SSSR	Single-Stator Single-Rotor
SSDR	Single-Stator Double-Rotor
DSSR	Double-Stator Single-Rotor
MSMR	Multi-Stator Multi-Rotor
AFIR	Axial-Flux Internal Rotor
YASA	Yokeless and Segmented Armature
PCB	Printed Circuit Board
SMC	Soft Magnetic Composite
FEM	Finite Element Method
FEA	Finite Element Analysis
MEC	Magnetic Equivalent Circuit
CFD	Computational Fluid Dynamics
ANN	Artificial Neural Network
GA	Genetic Algorithm
PSO	Particle Swarm Optimization
NSGA-II	Non-Dominated Sorting Genetic Algorithm II
HGA	Hybrid Genetic Algorithm
EGA	Elitist Genetic Algorithm
MOMVO	Multi-Objective Multi-Verse Optimization
LS	Least Squares
THD	Total Harmonic Distortion
EMF	Electromotive Force
EV	Electric Vehicle
BEV	Battery Electric Vehicle

PHEV	Plug-in Hybrid Electric Vehicle
CSI	Current Source Inverter
SVPWM	Space-Vector Pulse-Width Modulation
FOC	Field-Oriented Control
DTC	Direct Torque Control
MPC	Model Predictive Control
PI	Proportional Integral
SMO	Sliding Mode Observer
IPM	Interior Permanent Magnet
EDM	Electrical Discharge Machining
LPBF	Laser Powder Bed Fusion
NdFeB	Neodymium-Iron-Boron
TRV	Torque per Rotor Volume
HVACR	Heating, Ventilation, Air Conditioning, and Refrigeration
NEDC	New European Driving Cycle
US06	United States Supplemental Federal Test Procedure

References

1. Campbell, P. Principles of a permanent-magnet axial-field DC machine. *Proc. Inst. Electr. Eng.* **1975**, *121*, 1489–1494. [CrossRef]
2. Campbell, P. The magnetic circuit of an axial field D.C. electrical machine. *IEEE Trans. Magn.* **1975**, *11*, 1541–1543. [CrossRef]
3. Campbell, P.; Rosenberg, D.J.; Stanton, D.P. The computer design and optimization of axial-field permanent magnet motors. *IEEE Trans. Power Appar. Syst.* **1981**, *PAS-100*, 1490–1497. [CrossRef]
4. Havel, A.; Sobek, M.; Stepanec, L.; Strossa, J. Optimization of Permanent Magnet Parameters in Axial Flux Rotary Converter for HEV Drive. *Energies* **2022**, *15*, 724. [CrossRef]
5. Bloomberg. Axial Flux Motors: Mercedes and Ferrari's Edge in Electric Car Performance. 2022. Available online: https://www.bloomberg.com/news/articles/2022-08-17/mercedes-and-ferrari-s-edge-in-the-electric-age-high-end-motors (accessed on 4 July 2026).
6. Kumar, S.; Lipo, T.A.; Kwon, B.I. A 32,000 r/min Axial Flux Permanent Magnet Machine for Energy Storage with Mechanical Stress Analysis. *IEEE Trans. Magn.* **2016**, *52*, 8205004. [CrossRef]
7. Ouldhamrane, H.; Charpentier, J.-F.; Khoucha, F.; Zaoui, A.; Achour, Y.; Benbouzid, M. Optimal Design of Axial Flux Permanent Magnet Motors for Ship RIM-Driven Thruster. *Machines* **2022**, *10*, 932. [CrossRef]
8. Di Dio, V.; Cipriani, G.; Manno, D. Axial Flux Permanent Magnet Synchronous Generators for Pico Hydropower Application: A Parametrical Study. *Energies* **2022**, *15*, 6893. [CrossRef]
9. Shin, D.-Y.; Jung, M.-J.; Lee, K.-B.; Lee, K.-D.; Kim, W.-H. A Study on the Improvement of Torque Density of an Axial Slot-Less Flux Permanent Magnet Synchronous Motor for Collaborative Robot. *Energies* **2022**, *15*, 3464. [CrossRef]
10. Shao, L.Y.; Navaratne, R.; Popescu, M.; Liu, G.P. Design and Construction of Axial-Flux Permanent Magnet Motors for Electric Propulsion Applications—A Review. *IEEE Access* **2021**, *9*, 158998–159017. [CrossRef]
11. Min, Z.; Jing, L.; Wang, T.; Qu, R. A Partitioned Stator Flux Switching PM Machine with Strongly Coupled Flux Reversal Effect. *IEEE Trans. Transp. Electrif.* 2026, *in press*. [CrossRef]
12. Shukla, A.; Basak, S. Hybrid-Magnet based Multilayer Interior Permanent Magnet Synchronous Motor for Low-Voltage Small Pallet Electric Truck Application. *IEEE Trans. Consum. Electron.* 2026, *in press*.
13. Schäfer, A.; Pecha, U.; Parspour, N.; Kampker, A.; Born, H.; Hartmann, S.; Franke, J.; Baader, M.; Hahn, R. A Review of Electromagnetic Simulation and Modelling Approaches for the Research on Axial Flux Synchronous Machines. In Proceedings of the 2024 1st International Conference on Production Technologies and Systems for E-Mobility (EPTS), Bamberg, Germany, 5–6 June 2024. [CrossRef]
14. Samanta, P.; Mitikiri, S.B.; Sahay, P.K.; Srinivas, V.L. A comparative review of radial and axial Flux PMSMs: Innovations in topology, design, and control. *Frankl. Open* **2025**, *12*, 100341. [CrossRef]
15. Zhao, J.; Liu, X.; Wang, S.; Zheng, L. Review of Design and Control Optimization of Axial Flux PMSM in Renewable-energy Applications. *Chin. J. Mech. Eng.* **2023**, *36*, 45. [CrossRef]
16. Nishanth, F.; Van Verdeghem, J.; Severson, E.L. A Review of Axial Flux Permanent Magnet Machine Technology. *IEEE Trans. Ind. Appl.* **2023**, *59*, 3920–3933. [CrossRef]
17. Torkaman, H.; Ghaheri, A.; Keyhani, A. Design of Rotor Excited Axial Flux-Switching Permanent Magnet Machine. *IEEE Trans. Energy Convers.* **2018**, *33*, 1175–1183. [CrossRef]

18. Wang, X.G.; Zhao, M.; Zhou, Y.; Wan, Z.W.; Xu, W. Design and Analysis for Multi-Disc Coreless Axial-Flux Permanent-Magnet Synchronous Machine. *IEEE Trans. Appl. Supercond.* **2022**, *31*, 5203804. [CrossRef]
19. Polat, M.; Yildiz, A.; Akinci, R. Performance Analysis and Reduction of Torque Ripple of Axial Flux Permanent Magnet Synchronous Motor Manufactured for Electric Vehicles. *IEEE Trans. Magn.* **2021**, *57*, 1–9. [CrossRef]
20. Torres, J.; Pena, R.; Riedemann, J.; Tapia, J.; Moncada, R.; Jara, W.; Pesce, C. Direct power control strategy for an axial flux permanent magnet synchronous machine. *Electr. Eng.* **2020**, *102*, 481–491. [CrossRef]
21. Bouyahia, O.; Betin, F.; Yazidi, A. Fault-Tolerant Fuzzy Logic Control of a 6-Phase Axial Flux Permanent-Magnet Synchronous Generator. *Energies* **2022**, *15*, 1301. [CrossRef]
22. Zhao, J.; Zheng, L.; Wang, S.; Hua, M. Research on Deadbeat Current Prediction Vector Control System of Axial Flux Permanent Magnet Synchronous Motor for Electric Bus Based on Efficiency Optimal Torque Distribution Method. *IEEE Access* **2019**, *7*, 128384–128393. [CrossRef]
23. Shuaibu, I.; Wei, E.H.T.; Kannan, R.; Samaila, Y.A. Advancements in Axial Flux Permanent Magnet Machines Utilizing Coreless Technology: A Systematic Review. *Ain Shams Eng. J.* **2024**, *15*, 103091. [CrossRef]
24. Reyes, N.; Jimenez, M.; Hoffer, A.; Madariaga, C.; Gallardo, C.; Tapia, J.A.; Jara, W.; Degano, M. Structural Feasibility and Electromagnetic Analysis of an Ironless Rotor Axial Flux Permanent Magnet Synchronous Machine. In Proceedings of the 2023 IEEE Energy Conversion Congress and Exposition (ECCE), Nashville, TN, USA, 29 October–2 November 2023.
25. Zhu, X.; Zhang, L.; Xiao, X.; Lee, C.H.; Que, H. Adjustable-Flux Permanent Magnet Synchronous Motor Sensorless Drive System Based on Parameter-Sensitive Adaptive Online Decoupling Control Strategy. *IEEE Trans. Transp. Electrif.* **2022**, *9*, 501–511. [CrossRef]
26. Du, Y.; Huang, Y.; Guo, B.; Peng, F.; Dong, J. Semianalytical Model of Multiphase Halbach Array Axial Flux Permanent-Magnet Motor Considering Magnetic Saturation. *IEEE Trans. Transp. Electrif.* **2023**, *9*, 2891–2901. [CrossRef]
27. Hu, N.; Wang, Q.; Liu, S.; Gu, J.; Li, L.; Lyu, J. A Narrow Shape Double-Layer Microchannel Heat Sink (DL-MCHS) Designed for High-Power Laser Crystal. *Appl. Therm. Eng.* **2022**, *211*, 118456. [CrossRef]
28. European Commission. Circular Design and Manufacturing Techniques for Next-Generation Highly-Efficient Integrated Axial Flux Motor Drives for Electric Vehicles. 2023. Available online: https://climaflux.eu/ (accessed on 4 July 2026).
29. Hao, Z.; Ma, Y.; Wang, P.; Luo, G.; Chen, Y. A Review of Axial-Flux Permanent-Magnet Motors: Topological Structures, Design, Optimization and Control Techniques. *Machines* **2022**, *10*, 1178. [CrossRef]
30. Frank, Z.; Laksar, J. Analytical Design of Coreless Axial-Flux Permanent Magnet Machine with Planar Coils. *IEEE Trans. Energy Convers.* **2021**, *36*, 2348–2357. [CrossRef]
31. Si, J.; Wei, Y.; Nie, R.; Liang, J.; Gan, C.; Hu, Y. Analytical Modeling of Slotless Axial Flux Permanent Magnet Motor with Equidirectional Toroidal Winding. *IEEE Trans. Ind. Electron.* **2023**, *70*, 10420–10430. [CrossRef]
32. Huang, Y.K.; Zhou, T.; Dong, J.N.; Lin, H.Y.; Yang, H.; Cheng, M. Magnetic Equivalent Circuit Modeling of Yokeless Axial Flux Permanent Magnet Machine with Segmented Armature. *IEEE Trans. Magn.* **2014**, *50*, 8104204. [CrossRef]
33. Hwang, C.-C.; Li, P.-L.; Chuang, F.C.; Liu, C.-T.; Huang, K.-H. Optimization for Reduction of Torque Ripple in an Axial Flux Permanent Magnet Machine. *IEEE Trans. Magn.* **2009**, *45*, 1760–1763. [CrossRef]
34. Augusto, A.; Caetano, R.E. Design of a Yokeless Double Disc Axial Flux Motor for Light Electric Vehicles. *Frankl. Open* **2024**, *8*, 100166. [CrossRef]
35. Kahourzade, S.; Mahmoudi, A.; Ping, H.W.; Uddin, M.N. A Comprehensive Review of Axial-Flux Permanent-Magnet Machines. *Can. J. Electr. Comput. Eng.* **2014**, *37*, 19–33. [CrossRef]
36. Chaker, N.; Salah, I.; Tounsi, S.; Neji, R. Design of axial-flux motor for traction application. *J. Electromagn. Anal. Appl.* **2009**, *1*, 73–84. [CrossRef]
37. Cavagnino, A.; Lazzari, M.; Profumo, F.; Tenconi, A. Axial Flux Interior PM Synchronous Motor: Parameters Identification and Steady-State Performance Measurements. In Proceedings of the Conference Record of the 1999 IEEE Industry Applications Conference, Phoenix, AZ, USA, 3–7 October 1999.
38. Chen, Q.; Liang, D.; Liu, Y.; Wang, Q. Design and multi-object optimisation of axial flux interior PMSM for EV and HEV applications. *J. Eng.* **2017**, *2017*, 2215–2220. [CrossRef]
39. Aydin, M.; Huang, S.; Lipo, T. Axial flux permanent magnet disc machines: A review. In Proceedings of the Conference Record of SPEEDAM, Ravello, Italy, 11–14 June 2004.
40. Caricchi, F.; Crescimbini, F.; Santini, E. Basic principle and design criteria of axial-flux PM machines having counterrotating rotors. *IEEE Trans. Ind. Appl.* **1995**, *31*, 1062–1068. [CrossRef]
41. Guney, O.F.; Celik, A.; Bozkurt, A.F.; Erkan, K. Design and analysis of a high speed double-sided axial flux permanent magnet motor suspended vertically by magnetic bearings. *Int. J. Appl. Electromagn. Mech.* **2021**, *64*, S297–S310. [CrossRef]
42. Bruzinga, G.R.; Filho, A.J.S.; Pelizari, A. Analysis and design of 3 kW axial flux permanent magnet synchronous motor for electric car. *IEEE Lat. Am. Trans.* **2022**, *20*, 855–863. [CrossRef]

43. Kasim, M.; Irasari, P.; Hikmawan, M.F. Design, Simulation and Analysis of 3 kW Low Speed Axial Flux Permanent Magnet Generator. In Proceedings of the AIP Conference Proceedings, Surakarta, Indonesia, 11–12 November 2015.
44. Kurtuluş, F.; Akboy, E. Axial Flux Permanent Magnet Motor Design for Lightweight Applications. *Turk. J. Electr. Power Energy Syst.* **2020**, *5*, 2–9.
45. Habib, A.; Zainuri, M.A.A.M.; Che, H.S.; Ibrahim, A.A.; Abd Rahim, N.; Alaas, Z.M.; Ahmed, M.M.R. A systematic review on current research and developments on coreless axial-flux permanent-magnet machines. *IET Electr. Power Appl.* **2022**, *16*, 1095–1116. [CrossRef]
46. Baader, M.; Hahn, R.; Franke, J.; Kampker, A.; Born, H.; Hartmann, S.; Drexler, D.; Parspour, N.; Schäfer, A.; Pecha, U. The Production Process Chain of Axial Flux Motors: A Comparative Study. In Proceedings of the 2024 1st International Conference on Production Technologies and Systems for E-Mobility (EPTS), Bamberg, Germany, 5–6 June 2024. [CrossRef]
47. Alsuwian, T.; Habib, A.; Zainuri, M.A.A.M.; Ibrahim, A.A.; Tousizadeh, M.; Alhawari, A.R.; Almawgani, A.; Almasabi, S. Prototype development of a fully coreless multi-stage axial-flux permanent-magnet machine (AFPM). *Alex. Eng. J.* **2024**, *92*, 283–293. [CrossRef]
48. Vatani, M.; Lewis, D.; Eastham, J.; Ionel, D. Review of Coreless Axial Flux Permanent Magnet Machines with Applications Including Electric Aircraft Propulsion. *IEEE Trans. Transp. Electrif.* **2025**, *11*, 11358–11384. [CrossRef]
49. Sari, N.; Yudoyono, G.; Rohedi, A.Y.; Pramono, Y.H. Design and fabrication of rotor lateral shifting in the axial-flux permanent-magnet generator. *Int. J. Electr. Comput. Eng. (IJECE)* **2022**, *12*, 141–149. [CrossRef]
50. Syed, Q.A.S.; Hahn, I. Analysis of flux focusing double stator and single rotor axial flux permanent magnet motor. In Proceedings of the 2016 IEEE International Conference on Power Electronics, Drives and Energy Systems (PEDES), Trivandrum, India, 14–17 December 2016. [CrossRef]
51. Syed, Q.A.S.; Kurtovic, H.; Hahn, I. Double stator and single rotor type single-phase flux switching axial flux permanent magnet motor. In Proceedings of the 20th International Conference on Electrical Machines and Systems (ICEMS), Sydney, Australia, 11–14 August 2017. [CrossRef]
52. Syed, Q.A.S.; Hahn, I. Parametric Optimization of Flux Focusing Type Double Stator and Single Rotor Axial Flux Permanent Magnet Motor. In Proceedings of the 2018 IEEE International Magnetics Conference (INTERMAG), Singapore, 23–27 April 2018. [CrossRef]
53. Syed, Q.A.S.; Hahn, I. Influence of the Magnetic Bridges on the Flux Focusing Type Axial Flux Permanent Magnet Motor. In Proceedings of the 2018 IEEE Electrical Power and Energy Conference (EPEC), Toronto, ON, Canada, 10–11 October 2018. [CrossRef]
54. Sarıdağ, S.; Eker, M. Design of Double Stator Axial Flux Permanent Magnet Synchronous Motor (DS-AFPMSM). *J. New Results Eng. Nat. Sci.* **2025**, *2024*, 30–46.
55. Aydin, M.; Huang, S.; Lipo, T.A. Design and 3D electromagnetic field analysis of non-slotted and slotted TORUS type axial flux surface mounted permanent magnet disc machines. *IEEE Trans. Magn.* **2002**, *38*, 1299–1302.
56. Larbi, B.; Hatti, M.; Kouzi, K.; Ghadbane, A. Axial flux machine with non-slotted torus-ns rotor type. Design and analysis. *Electr. Eng. Electromech.* **2023**, *6*, 10–15. [CrossRef]
57. Mahmoudi, A.; Rahim, N.A.; Ping, H.W. A Comparison Between the TORUS and AFIR Axial-Flux Permanent-Magnet Machines. In Proceedings of the 1st IEEE Conference on Industrial Electronics and Applications, Singapore, 24–26 May 2006.
58. Mirzahosseini, R.; Darabi, A.; Assili, M. An analytical formula for selecting the feeding voltage and frequency in a TORUS-type nonslotted axial flux permanent magnet machine design. *Turk. J. Electr. Eng. Comput. Sci.* **2009**, *27*, 2295–2308.
59. Fei, E.; Luk, P.C.K. A new axial flux permanent magnet Segmented-Armature-Torus machine for flywheel energy storage system. *IEEE Trans. Magn.* **2008**, *44*, 4076–4079. [CrossRef]
60. Mahmoudi, A.; Rahim, N.A.; Ping, H.W. Design, analysis, and prototyping of an axial-flux permanent magnet motor based on axial-flux coreless stator windings. *IEEE Trans. Magn.* **2011**, *47*, 4760–4767.
61. Vatani, M.; Eastham, J.F.; Ionel, D.M. Multi-Disk Coreless Axial Flux Permanent Magnet Motors with Halbach PM Array Rotors. In Proceedings of the IEEE Energy Conversion Congress and Exposition (ECCE), Phoenix, AZ, USA, 20–24 October 2024.
62. Habib, A.; Che, H.S.; Mohamed, F. A fully coreless Multi-Stator Multi-Rotor (MSMR) AFPM generator with combination of conventional and Halbach magnet arrays. *Alex. Eng. J.* **2020**, *59*, 589–600. [CrossRef]
63. Kou, B.; Huang, X. Comparative Analysis of Coreless Multidisc Axial Flux Permanent Magnet Motor. In Proceedings of the 2022 IEEE 5th International Electrical and Energy Conference (CIEEC), Nangjing, China, 27–29 May 2022. [CrossRef]
64. Si, J.K.; Zhang, T.X.; Hu, Y.H.; Gan, C.; Li, Y.S. An Axial-Flux Dual-Rotor Slotless Permanent Magnet Motor with Novel Equidirectional Toroidal Winding. *IEEE Trans. Energy Convers.* **2022**, *37*, 1752–1763. [CrossRef]
65. Kaiser, B.; Parspour, N. Transverse Flux Machine—A Review. *IEEE Access* **2022**, *10*, 18395–18419. [CrossRef]
66. Kalender, O.; Ege, Y.; Nazlibilek, S. Design and determination of stator geometry for axial flux permanent magnet free rod rotor synchronous motor. *Measurement* **2011**, *44*, 1753–1760. [CrossRef]

67. Carpi, T.; Bonnet, M.; Touhami, S.; Lefevre, Y.; Llibre, J.F. Unified Sizing Model Approach for Radial and Axial Flux Permanent Magnet Machines. In Proceedings of the 24th International Conference on Electrical Machines (ICEM), Gothenburg, Sweden, 23–26 August 2020. [CrossRef]
68. Zhao, J.L.; Lu, Z.L.; Han, Q.F.; Wang, L.; Lin, M.Y. An Overview on Development of Axial Flux Permanent Magnet Motor System and the Key Technology. *Proc. CSEE* **2022**, *42*, 2744–2764.
69. Huang, S.R.; Luo, J.; Leonardi, F.; Lipo, T.A. A general approach to sizing and power density equations for comparison of electrical machines. *IEEE Trans. Ind. Appl.* **1998**, *34*, 92–97. [CrossRef]
70. Chen, A.Y.; Nilssen, R.; Nysveen, A. Performance Comparisons Among Radial-Flux, Multistage Axial-Flux, and Three-Phase Transverse-Flux PM Machines for Downhole Applications. *IEEE Trans. Ind. Appl.* **2010**, *46*, 779–789. [CrossRef]
71. Huang, S.; Luo, J.; Leonardi, F.; Lipo, T.A. A Comparison of Power Density for Axial Flux Machines Based on General Purpose Sizing Equations. *IEEE Trans. Energy Convers.* **1999**, *14*, 185–192. [CrossRef]
72. Pyrhönen, J.; Jokinen, T.; Hrabovcová, V. *Design of Rotating Electrical Machines*; John Wiley & Sons: Chichester, UK, 2013. [CrossRef]
73. Gadiyar, N.; Bohach, G.; Nahin, M.M.; Van de Ven, J.; Severson, E.L.; Nishanth, F. Development of an Integrated Electro-Hydraulic Machine to Electrify Off-Highway Vehicles. *IEEE Trans. Ind. Appl.* **2022**, *58*, 6163–6174. [CrossRef]
74. Capponi, F.G.; Donato, G.D.; Caricchi, F. Recent Advances in Axial-Flux Permanent-Magnet Machine Technology. *IEEE Trans. Ind. Appl.* **2012**, *48*, 2190–2205. [CrossRef]
75. Wang, M.Q.; Tong, C.D.; Song, Z.Y.; Liu, J.Q.; Zheng, P. Performance Analysis of an Axial Magnetic-Field-Modulated Brushless Double-Rotor Machine for Hybrid Electric Vehicles. *IEEE Trans. Ind. Electron.* **2018**, *66*, 806–817. [CrossRef]
76. Yesilbag, E.; Ertugrul, Y.; Ergene, L. Axial flux PM BLDC motor design methodology and comparison with a radial flux PM BLDC motor. *Turk. J. Electr. Eng. Comput. Sci.* **2017**, *25*, 3455–3467. [CrossRef]
77. Kim, J.H.; Choi, W.; Sarlioglu, B. Closed-Form Solution for Axial Flux Permanent-Magnet Machines with a Traction Application Study. *IEEE Trans. Ind. Appl.* **2016**, *52*, 1775–1784. [CrossRef]
78. Wang, C.; Zhang, Z.R.; Liu, Y.; Geng, W.W.; Gao, H.M. Effect of Slot-Pole Combination on the Electromagnetic Performance of Ironless Stator AFPM Machine with Concentrated Windings. *IEEE Trans. Energy Convers.* **2020**, *35*, 1098–1109. [CrossRef]
79. Dwivedi, A.; Singh, S.K.; Srivastava, R.K. Analysis and Performance Evaluation of Axial Flux Permanent Magnet Motors. *IEEE Trans. Ind. Appl.* **2018**, *54*, 1765–1772. [CrossRef]
80. Taran, N.; Heins, G.; Rallabandi, V.; Patterson, D.; Ionel, D.M. Evaluating the Effects of Electric and Magnetic Loading on the Performance of Single- and Double-Rotor Axial-Flux PM Machines. *IEEE Trans. Ind. Appl.* **2020**, *56*, 3488–3497. [CrossRef]
81. Nishanth, F.; Johnson, M.; Severson, E.L. A Review of Thermal Analysis and Management of Power Dense Electric Machines. In Proceedings of the IEEE International Electric Machines & Drives Conference (IEMDC), Hartford, CT, USA, 17–20 May 2021.
82. Nishanth, F.; Verdeghem, J.V.; Severson, E.L. Recent Advances in Analysis and Design of Axial Flux Permanent Magnet Electric Machines. In Proceedings of the IEEE Energy Conversion Congress and Exposition (ECCE), Vancouver, BC, Canada, 10–14 October 2021.
83. Credo, A.; Tursini, M.; Villani, M.; Di Lodovico, C.; Orlando, M.; Frattari, F. Axial Flux PM In-Wheel Motor for Electric Vehicles: 3D Multiphysics Analysis. *Energies* **2021**, *14*, 2107. [CrossRef]
84. Jung, J.W.; Park, H.I.; Hong, J.P.; Lee, B.H. A Novel Approach for 2-D Electromagnetic Field Analysis of Surface Mounted Permanent Magnet Synchronous Motor Taking into Account Axial End Leakage Flux. *IEEE Trans. Magn.* **2017**, *53*, 8208104. [CrossRef]
85. Khatab, M.; Zhu, Z.Q.; Li, H.; Lipo, T.A. Comparative study of novel axial flux magnetically geared and conventional axial flux permanent magnet machines. *CES Trans. Electr. Mach. Syst.* **2019**, *2*, 392–398. [CrossRef]
86. Scheerlinck, B.; Gersem, H.D.; Sergeant, P. 3-D eddy current and fringing-flux distribution in an axial-flux permanent-magnet synchronous machine with stator in laminated iron or SMC. *IEEE Trans. Magn.* **2015**, *51*, 1–4. [CrossRef]
87. Nguyen, T.D.; Tseng, K.-J.; Zhang, S.; Nguyen, H.T. A Novel Axial Flux Permanent-Magnet Machine for Flywheel Energy Storage System: Design and Analysis. *IEEE Trans. Ind. Electron.* **2011**, *58*, 3784–3794. [CrossRef]
88. Benlamine, R.; Dubas, F.; Randi, S.-A.; Lhotellier, D.; Espanet, C. Modeling of an axial-flux interior PMs machine for an automotive application using magnetic equivalent circuit. In Proceedings of the 2015 18th International Conference on Electrical Machines and Systems (ICEMS), Pattaya, Thailand, 25–28 October 2015. [CrossRef]
89. Hemeida, A.; Lehikoinen, A.; Rasilo, P.; Vansompel, H.; Belahcen, A.; Arkkio, A.; Sergeant, P. A Simple and Efficient Quasi-3D Magnetic Equivalent Circuit for Surface Axial Flux Permanent Magnet Synchronous Machines. *IEEE Trans. Ind. Electron.* **2019**, *66*, 8318–8333. [CrossRef]
90. Li, N.; Zhu, J.; Lin, M.; Yang, G.; Kong, Y.; Hao, L. Analysis of Axial Field Flux-Switching Memory Machine Based on 3-D Magnetic Equivalent Circuit Network Considering Magnetic Hysteresis. *IEEE Trans. Magn.* **2019**, *55*, 1–4. [CrossRef]
91. Tak, B.-O.; Ro, J.-S. Analysis and Design of an Axial Flux Permanent Magnet Motor for in-Wheel System Using a Novel Analytical Method Combined with a Numerical Method. *IEEE Access* **2020**, *8*, 203994–204011. [CrossRef]

92. Tong, W.; Wang, S.; Dai, S.; Wu, S.; Tang, R. A Quasi-Three-Dimensional Magnetic Equivalent Circuit Model of a Double-Sided Axial Flux Permanent Magnet Machine Considering Local Saturation. *IEEE Trans. Energy Convers.* **2018**, *33*, 2163–2173. [CrossRef]
93. Maloberti, O.; Figueredo, R.; Marchand, C.; Choua, Y.; Condamin, D.; Kobylanski, L.; Bommé, E. 3-D–2-D Dynamic Magnetic Modeling of an Axial Flux Permanent Magnet Motor with Soft Magnetic Composites for Hybrid Electric Vehicles. *IEEE Trans. Magn.* **2014**, *50*, 1–11. [CrossRef]
94. Yoshida, Y.; Nakamura, K.; Ichinokura, O. A Method for Calculating Eddy Current Loss Distribution Based on Reluctance Network Analysis. *IEEE Trans. Magn.* **2011**, *47*, 4155–4158. [CrossRef]
95. Hemeida, A.; Sergeant, P.; Vansompel, H. Comparison of Methods for Permanent Magnet Eddy-Current Loss Computations with and Without Reaction Field Considerations in Axial Flux PMSM. *IEEE Trans. Magn.* **2015**, *51*, 1–11. [CrossRef]
96. Ojaghlu, P.; Vahedi, A.; Totoonchian, F. Magnetic equivalent circuit modelling of ring winding axial flux machine. *IET Electr. Power Appl.* **2018**, *12*, 293–300. [CrossRef]
97. Hou, J.; Geng, W.; Li, Q.; Zhang, Z. 3-D Equivalent Magnetic Network Modeling and FEA Verification of a Novel Axial-Flux Hybrid-Excitation In-wheel Motor. *IEEE Trans. Magn.* **2021**, *57*, 1–12. [CrossRef]
98. Asfirane, S.; Hlioui, S.; Mezani, S.; Amara, Y.; De La Barriere, O.; Barakat, G.; Gabsi, M. Scalar Magnetic Potential Interpolation for Non-Conformal Meshing in Mesh-Based Generated Reluctance Networks. *IEEE Trans. Magn.* **2019**, *55*, 1–8. [CrossRef]
99. Bruzzese, C.; Zito, D.; Tessarolo, A. Finite reluctance approach: A systematic method for the construction of magnetic network-based dynamic models of electrical machines. In Proceedings of the 2014 AEIT Annual Conference, Trieste, Italy, 18–19 September 2014. [CrossRef]
100. Taran, N.; Klink, D.; Heins, G.; Rallabandi, V.; Patterson, D.; Ionel, D.M. A Comparative Study of Yokeless and Segmented Armature Versus Single Sided Axial Flux PM Machine Topologies for Electric Traction. *IEEE Trans. Ind. Appl.* **2022**, *58*, 325–335. [CrossRef]
101. Benlamine, R.; Dubas, F.; Randi, S.-A.; Lhotellier, D.; Espanet, C. 3-D Numerical Hybrid Method for PM Eddy-Current Losses Calculation: Application to Axial-Flux PMSMs. *IEEE Trans. Magn.* **2015**, *51*, 1–10. [CrossRef]
102. Vansompel, H.; Sergeant, P.; Dupre, L. A Multilayer 2-D–2-D Coupled Model for Eddy Current Calculation in the Rotor of an Axial-Flux PM Machine. *IEEE Trans. Energy Convers.* **2012**, *27*, 784–791. [CrossRef]
103. Egea, A.; Almandoz, G.; Poza, J.; Ugalde, G.; Escalada, A.J. Axial-Flux-Machine Modeling with the Combination of FEM-2-D and Analytical Tools. *IEEE Trans. Ind. Appl.* **2012**, *48*, 1318–1326. [CrossRef]
104. Gulec, M.; Aydin, M. Implementation of different 2D finite element modelling approaches in axial flux permanent magnet disc machines. *IET Electr. Power Appl.* **2018**, *12*, 195–202. [CrossRef]
105. Tiegna, H.; Amara, Y.; Barakat, G. A New Quasi-3-D Analytical Model of Axial Flux Permanent Magnet Machines. *IEEE Trans. Magn.* **2014**, *50*, 817–820. [CrossRef]
106. Kim, K.-H.; Woo, D.-K. Novel Quasi-Three-Dimensional Modeling of Axial Flux In-Wheel Motor with Permanent Magnet Skew. *IEEE Access* **2022**, *10*, 98842–98854. [CrossRef]
107. Schäfer, A.; Pecha, U.; Kaiser, B.; Schmid, M.; Parspour, N. Accelerated 3D FEA of an Axial Flux Machine by Exclusively Using the Magnetic Scalar Potential. *Energies* **2023**, *16*, 6596. [CrossRef]
108. D'Angelo, J.; Chari, M.; Campbell, P. Three-Dimensional Finite Element Solution for a Permanent Magnet Axial-Field Machine. *IEEE Trans. Power Appar. Syst.* **1983**, *PAS-102*, 83–90.
109. Locment, F.; Semail, E.; Piriou, F. Design and study of a multiphase axial-flux machine. *IEEE Trans. Magn.* **2006**, *42*, 1427–1430. [CrossRef]
110. Ajily, E.; Abbaszadeh, K.; Ardebili, M. Three-Dimensional Field Reconstruction Method for Modeling Axial Flux Permanent Magnet Machines. *IEEE Trans. Energy Convers.* **2015**, *30*, 199–207. [CrossRef]
111. Park, H.-J.; Jung, H.-K.; Jung, S.-Y.; Chae, Y.-H.; Woo, D.-K. Field Reconstruction Method in Axial Flux Permanent Magnet Motor with Overhang Structure. *IEEE Trans. Magn.* **2017**, *53*, 1–4. [CrossRef]
112. Lim, D.K.; Woo, D.K.; Kim, I.W.; Ro, J.S.; Jung, H.K. Cogging Torque Minimization of a Dual-Type Axial-Flux Permanent Magnet Motor Using a Novel Optimization Algorithm. *IEEE Trans. Magn.* **2013**, *49*, 5106–5111. [CrossRef]
113. Fard, J.R.; Ardebili, M. Design and prototyping of the novel axial flux-switching permanent-magnet motor. *COMPEL* **2018**, *37*, 890–910. [CrossRef]
114. Lok, C.L.; Vengadaesvaran, B.; Ramesh, S. Implementation of hybrid pattern search-genetic algorithm into optimizing axial-flux permanent magnet coreless generator (AFPMG). *Electr. Eng.* **2017**, *99*, 751–761. [CrossRef]
115. Verkroost, L.; Vansompel, H.; De Belie, F.; Sergeant, P. Comparison Between Two Fault Tolerant Deadbeat Controllers under Partial Demagnetization Faults in Permanent Magnet Synchronous Machines. In Proceedings of the 24th International Conference on Electrical Machines (ICEM), Gothenburg, Sweden, 23–26 August 2020.
116. Meo, S.; Zohoori, A.; Vahedi, A. Optimal design of permanent magnet flux switching generator for wind applications via artificial neural network and multi-objective particle swarm optimization hybrid approach. *Energy Convers. Manag.* **2016**, *110*, 230–239. [CrossRef]

117. Fard, J.R.; Ardebili, M. Optimal Design and Analysis of the Novel Low Cogging Torque Axial Flux-Switching Permanent-Magnet Motor. *Electr. Power Compon. Syst.* **2018**, *46*, 1330–1339. [CrossRef]
118. Patel, A.N.; Suthar, B.N. Cogging Torque Reduction of Sandwiched Stator Axial Flux Permanent Magnet Brushless DC Motor using Magnet Notching Technique. *Int. J. Eng.* **2019**, *32*, 940–946. [CrossRef]
119. Wang, S.; Zhao, J.; Liu, T.; Hua, M. Adaptive robust control system for axial flux permanent magnet synchronous motor of electric medium bus based on torque optimal distribution method. *Energies* **2019**, *12*, 4681. [CrossRef]
120. Shariati, O.; Behnamfar, A.; Potter, B. An Integrated Elitist Approach to the Design of Axial Flux Permanent Magnet Synchronous Wind Generators (AFPMWG). *Energies* **2022**, *15*, 3262. [CrossRef]
121. Deng, W.Z.; Zuo, S.G. Noise reduction of axial-flux motors by combining various pole-arc coefficients and circumferential shifting of permanent magnets: Analytical approach. *IET Electr. Power Appl.* **2019**, *13*, 951–957. [CrossRef]
122. Sun, S.; Jiang, F.; Li, T.; Xu, B.; Yang, K. Comparison of a Multi-Stage Axial Flux Permanent Magnet Machine with Different Stator Core Materials. *IEEE Trans. Appl. Supercond.* **2020**, *30*, 1–6. [CrossRef]
123. Sun, X.; Shi, Z.; Lei, G.; Guo, Y.; Zhu, J. Analysis and Design Optimization of a Permanent Magnet Synchronous Motor for a Campus Patrol Electric Vehicle. *IEEE Trans. Veh. Technol.* **2019**, *68*, 10535–10544. [CrossRef]
124. Levent, A.H.; Lordoglu, A.; Aydeniz, M.G. Design and Optimization of Permanent Magnet Synchronous Motor for Electric Vehicle Applications. In Proceedings of the 2020 2nd Global Power, Energy and Communication Conference (GPECOM), Izmir, Turkey, 20–23 October 2020. [CrossRef]
125. Gulec, M.; Aydin, M. Design and Optimization of an Axial Flux Permanent Magnet Assisted Eddy Current Brake. In Proceedings of the 12th International Conference on Electrical and Electronics Engineering (ELECO), Bursa, Turkey, 26–28 November 2020.
126. Abd-Rabou, A.S.; Marei, M.I.; El-Sattar, A.A.; Basha, M.A. Multiobjective Design optimization of Axial Flux Permanent Magnet Brushless DC Micromotor Using Response Surface Methodology and Multi-Verse optimization Algorithm. In Proceedings of the IEEE Jordan International Joint Conference on Electrical Engineering and Information Technology (JEEIT), Amman, Jordan, 9–11 April 2019. [CrossRef]
127. Zhu, J.; Li, G.H.; Cao, D.; Zhang, Z.Y. Voltage regulation Rate and THD optimization analysis of coreless axial flux PM synchronous generator for wind power generation. *IEEJ Trans. Electr. Electron. Eng.* **2019**, *14*, 1485–1493. [CrossRef]
128. Rostami, N. Particle swarm optimization approach to optimal design of an AFPM traction machine for different driving conditions. *Turk. J. Electr. Eng. Comput. Sci.* **2019**, *27*, 3234–3246. [CrossRef]
129. Chakkarapani, K.; Thangavelu, T.; Dharmalingam, K.; Thandavarayan, P. Multiobjective design optimization and analysis of magnetic flux distribution for slotless permanent magnet brushless DC motor using evolutionary algorithms. *J. Magn. Magn. Mater.* **2019**, *476*, 524–537. [CrossRef]
130. Guo, B.; Du, Y.; Djelloul-Khedda, Z.; Peng, F.; Dong, J.; Huang, Y.; Dubas, F.; Boughrara, K. Nonlinear Semianalytical Model for Axial Flux Permanent-Magnet Machine. *IEEE Trans. Ind. Electron.* **2022**, *69*, 9804–9816. [CrossRef]
131. Taqavi, O.; Mirimani, S.M. Design Aspects, Winding Arrangements and Applications of Printed Circuit Board Motors: Comprehensive Review. *IET Electr. Power Appl.* **2020**, *14*, 1505–1518. [CrossRef]
132. Tsai, M.-F.; Lee, T.-C.; Tseng, C.-S.; Syu, W.-S.; Chen, Y.-Y.; Peng, W.-Y. Vector Control of Current Source Inverter-Fed Axial-Flux Permanent Magnet Motors with Space Vector Pulse Width Modulation. In Proceedings of the 2014 IEEE 23rd International Symposium on Industrial Electronics (ISIE), Istanbul, Turkey, 1–4 June 2014. [CrossRef]
133. Noh, M.D.; Kim, J.; Park, Y.-W. Comparisons of Concentrated Printed-Circuit Stator Windings for Axial Flux Permanent Magnet Machines. In Proceedings of the IEEE/ASME International Conference on Advanced Intelligent Mechatronics (AIM), Hong Kong, China, 8–12 July 2019. [CrossRef]
134. Paul, S.; Farshadnia, M.; Pouramin, A.; Fletcher, J.; Chang, J. Comparative Analysis of Wave Winding Topologies and Performance Characteristics in Ultra-Thin Printed Circuit Board Axial-Flux PM Machine. *IET Electr. Power Appl.* **2019**, *13*, 694–701. [CrossRef]
135. Neethu, S.; Nikam, S.P.; Pal, S.; Wankhede, A.K.; Fernandes, B.G. Performance Comparison Between PCB-Stator and Laminated-Core-Stator-Based Designs of Axial Flux Permanent Magnet Motors for High-Speed Low-Power Applications. *IEEE Trans. Ind. Electron.* **2020**, *67*, 5269–5277. [CrossRef]
136. Wang, Y.; Lu, J.; Liu, C.; Lei, G.; Guo, Y.; Zhu, J. Development of a High-Performance Axial Flux PM Machine With SMC Cores for Electric Vehicle Application. *IEEE Trans. Magn.* **2019**, *55*, 1–4. [CrossRef]
137. Wang, Z.; Masaki, R.; Morinaga, S.; Enomoto, Y.; Itabashi, H.; Ito, M.; Tanigawa, S. Development of an Axial Gap Motor with Amorphous Metal Cores. *IEEE Trans. Ind. Appl.* **2011**, *47*, 1293–1299. [CrossRef]
138. Kim, C.-W.; Jang, G.-H.; Kim, J.-M.; Ahn, J.-H.; Baek, C.-H.; Choi, J.-Y. Comparison of Axial Flux Permanent Magnet Synchronous Machines with Electrical Steel Core and Soft Magnetic Composite Core. *IEEE Trans. Magn.* **2017**, *53*, 1–4. [CrossRef]
139. Schäfer, A.; Baranowski, M.; Springmann, M.; Hof, L.; Frölich, F.; Peter, A.; Parspour, N.; Fleischer, J.; Middendorf, P.; Kärger, L.; et al. Design concept of a repairable YASA axial flux machine with a hybrid cooling system. In Proceedings of the 12th International Conference on Power Electronics, Machines and Drives (PEMD 2023), Brussels, Belgium, 23–24 October 2023. [CrossRef]

140. Liben, M.; Ludois, D.C. Analytical Design and Experimental Testing of a Self-Cooled, Toroidally Wound Ring Motor with Integrated Propeller for Electric Rotorcraft. *IEEE Trans. Ind. Appl.* **2021**, *57*, 2342–2353. [CrossRef]
141. Ghaheri, A.; Mohammadi Ajamloo, A.; Torkaman, H.; Afjei, E. Design, Modelling and Optimisation of a Slot-Less Axial Flux Permanent Magnet Generator for Direct-Drive Wind Turbine Application. *IET Electr. Power Appl.* **2020**, *14*, 1327–1338. [CrossRef]
142. Nishanth, F.N.; Goodall, A.D.; Todd, I.; Severson, E.L. Characterization of an Axial Flux Machine with an Additively Manufactured Stator. *IEEE Trans. Energy Convers.* **2023**, *38*, 2717–2729. [CrossRef]
143. Sahin, F. Design and Development of a High-Speed Axial-Flux Permanent-Magnet Machine. Ph.D. Thesis, Eindhoven University of Technology, Eindhoven, The Netherlands, 2001.
144. Shah Syed, Q.A.; Solovieva, V.; Hahn, I. Magnetization Characteristics and Loss Measurements of the Axial Flux Permanent Magnet Motor's Stator. In Proceedings of the IEEE International Electric Machines & Drives Conference (IEMDC), San Diego, CA, USA, 12–15 May 2019. [CrossRef]
145. Bonnet, M.; Lefevre, Y.; Llibre, J.; Harribey, D.; Defay, F.; Sadowski, N. 3D Magnetic Field Model of a Permanent Magnet Ironless Axial Flux Motor with Additively Manufactured Non-Active Parts. In Proceedings of the International Symposium on Electromagnetic Fields (ISEF), Nancy, France, 29–31 August 2019. [CrossRef]
146. Tiismus, H.; Kallaste, A.; Vaimann, T.; Rassolkin, A.; Belahcen, A. Additive Manufacturing of Prototype Axial Flux Switched Reluctance Machine. In Proceedings of the International Workshop on Electric Drives, Moscow, Russia, 27–29 January 2021. [CrossRef]
147. Wanjiku, J.; Khan, M.A.; Barendse, P.S.; Pillay, P. Influence of Slot Openings and Tooth Profile on Cogging Torque in Axial-Flux PM Machines. *IEEE Trans. Ind. Electron.* **2015**, *62*, 7578–7589. [CrossRef]
148. Letelier, A.B.; Gonzalez, D.A.; Tapia, J.A.; Wallace, R.; Valenzuela, M.A. Cogging Torque Reduction in an Axial Flux PM Machine via Stator Slot Displacement and Skewing. *IEEE Trans. Ind. Appl.* **2007**, *43*, 685–693. [CrossRef]
149. Aydin, M.; Zhu, Z.Q.; Lipo, T.A.; Howe, D. Minimization of Cogging Torque in Axial-Flux Permanent-Magnet Machines: Design Concepts. *IEEE Trans. Magn.* **2007**, *43*, 3614–3622. [CrossRef]
150. Vansompel, H.; Sergeant, P.; Dupre, L. Effect of Segmentation on Eddy-Current Loss in Permanent Magnets of Axial-Flux PM Machines Using a Multilayer-2D Coupled Model. In Proceedings of the International Conference on Electrical Machines, Marseille, France, 2–5 September 2012. [CrossRef]
151. Vansompel, H.; Sergeant, P.; Dupre, L.; Van den Bossche, A. Axial-Flux PM Machines with Variable Air Gap. *IEEE Trans. Ind. Electron.* **2014**, *61*, 730–737. [CrossRef]
152. Javadi, S.; Mirsalim, M. A Coreless Axial-Flux Permanent-Magnet Generator for Automotive Applications. *IEEE Trans. Magn.* **2008**, *44*, 4591–4598. [CrossRef]
153. Wiltuschnig, I.P.; Eckert, P.R.; Dorrell, D.G.; Flores Filho, A.F. A Study of the Influence of Quasi-Halbach Arrays on a Torus Machine. *IEEE Trans. Magn.* **2016**, *52*, 1–4. [CrossRef]
154. Zhang, Z.; Wang, C.; Geng, W. Design and Optimization of Halbach-Array PM Rotor for High-Speed Axial-Flux Permanent Magnet Machine with Ironless Stator. *IEEE Trans. Ind. Electron.* **2020**, *67*, 7269–7279. [CrossRef]
155. Neethu, S.; Nikam, S.P.; Singh, S.; Pal, S.; Wankhede, A.K.; Fernandes, B.G. High-Speed Coreless Axial-Flux Permanent-Magnet Motor with Printed Circuit Board Winding. *IEEE Trans. Ind. Appl.* **2019**, *55*, 1954–1962. [CrossRef]
156. Aydin, M.; Gulec, M. Reduction of Cogging Torque in Double-Rotor Axial-Flux PM Disk Motors: A Review of Cost-Effective Magnet-Skewing Techniques with Experimental Verification. *IEEE Trans. Ind. Electron.* **2014**, *61*, 5025–5034. [CrossRef]
157. Aydin, M.; Gulec, M. A New Coreless Axial Flux Interior Permanent Magnet Synchronous Motor with Sinusoidal Rotor Segments. *IEEE Trans. Magn.* **2016**, *52*, 1–4. [CrossRef]
158. Shokri, M.; Rostami, N.; Behjat, V.; Pyrhonen, J.; Rostami, M. Comparison of Performance Characteristics of Axial-Flux Permanent-Magnet Synchronous Machine with Different Magnet Shapes. *IEEE Trans. Magn.* **2015**, *51*, 1–6. [CrossRef]
159. Ali, S.; Rubino, G.; Ciprini, L.; Ali, R.; Marignetti, F. Comparative Study Among Different Rotor Topologies of Axial Flux Permanent Magnet Machines. In Proceedings of the Second International Conference on Sustainable Mobility Applications, Renewables and Technology (SMART), Cassino, Italy, 23–25 November 2022. [CrossRef]
160. Ali, S.; Ikram, J.; Devereux, C.P.; Bukhari, S.S.H.; Khan, S.A.; Khan, N.; Ro, J.-S. Reduction of Cogging Torque in AFPM Machine Using Elliptical-Trapezoidal-Shaped Permanent Magnet. *Appl. Comput. Electromagn. Soc. J.* **2021**, *36*, 1090–1098. [CrossRef]
161. Vansompel, H.; Sergeant, P. Extended End-Winding Cooling Insert for High Power Density Electric Machines with Concentrated Windings. *IEEE Trans. Energy Convers.* **2020**, *35*, 948–955. [CrossRef]
162. Caricchi, F.; Capponi, F.G.; Crescimbini, F.; Solero, L. Experimental study on reducing cogging torque and no-load power loss in axial-flux permanent-magnet machines with slotted winding. *IEEE Trans. Ind. Appl.* **2004**, *40*, 1066–1075. [CrossRef]
163. Van Damme, J.; Vansompel, H.; Crevecoeur, G. Anodized Aluminum Foil Winding Axial Flux Machine for Direct-Drive Robotic Applications. *IEEE Trans. Ind. Electron.* **2023**, *70*, 10409–10419. [CrossRef]
164. Polikarpova, M.; Lindh, P.; Gerada, C.; Rilla, M.; Naumanen, V.; Pyrhonen, J. Thermal Effects of Stator Potting in an Axial-Flux Permanent Magnet Synchronous Generator. *Appl. Therm. Eng.* **2015**, *75*, 421–429. [CrossRef]

165. Lindh, P.; Petrov, I.; Jaatinen-Varri, A.; Gronman, A.; Martinez-Iturralde, M.; Satrustegui, M.; Pyrhonen, J. Direct Liquid Cooling Method Verified with an Axial-Flux Permanent-Magnet Traction Machine Prototype. *IEEE Trans. Ind. Electron.* **2017**, *64*, 6086–6095. [CrossRef]
166. Meier, M.; Strangas, E. Improved Cooling for a High-Speed Axial-Flux Machine Using Soft Magnetic Composites. In Proceedings of the IEEE Energy Conversion Congress and Exposition (ECCE), Detroit, MI, USA, 9–13 October 2022. [CrossRef]
167. Bi, Y.; Chai, F.; Chen, L. The study of cooling enhancement in axial flux permanent magnet motors for electric vehicles. *IEEE Trans. Ind. Appl.* **2021**, *57*, 4831–4839. [CrossRef]
168. Roy, R.; Ramasami, S.; Chokkalingam, L.N. Review on Thermal Behavior and Cooling Aspects of Axial Flux Permanent Magnet Motors—A Mechanical Approach. *IEEE Access* **2023**, *11*, 6822–6841. [CrossRef]
169. Rahman, K.M.; Patel, N.R.; Ward, T.G.; Nagashima, J.M.; Caricchi, F.; Crescimbini, F. Application of Direct-Drive Wheel Motor for Fuel Cell Electric and Hybrid Electric Vehicle Propulsion System. *IEEE Trans. Ind. Appl.* **2006**, *42*, 1185–1192. [CrossRef]
170. Marcolini, F.; De Donato, G.; Capponi, F.G.; Caricchi, F. Direct Oil Cooling of End-Windings in Torus-Type Axial-Flux Permanent-Magnet Machines. *IEEE Trans. Ind. Appl.* **2021**, *57*, 2378–2386. [CrossRef]
171. Fawzal, A.S.; Cirstea, R.M.; Gyftakis, K.N.; Woolmer, T.J.; Dickison, M.; Blundell, M. Fan Performance Analysis for Rotor Cooling of Axial Flux Permanent Magnet Machines. *IEEE Trans. Ind. Appl.* **2017**, *53*, 3295–3304. [CrossRef]
172. Chuan, H.; Burke, R.; Wu, Z. A Comparative Study on Different Cooling Topologies for Axial Flux Permanent Magnet Machine. In Proceedings of the IEEE Vehicle Power and Propulsion Conference (VPPC), Hanoi, Vietnam, 14–17 October 2019. [CrossRef]
173. Tsunata, R.; Takemoto, M.; Imai, J.; Saito, T.; Ueno, T. Comparison of Thermal Characteristics in Various Aspect Ratios of Radial-Flux and Axial-Flux Permanent Magnet Machines. *IEEE Trans. Ind. Appl.* **2022**, *59*, 3353–3367. [CrossRef]
174. Gora, R.; Biswas, R.; Garg, R.K.; Nangia, U. Field Oriented Control of Permanent Magnet Synchronous Motor (PMSM) Driven Electric Vehicle and Its Performance Analysis. In Proceedings of the 2021 IEEE 4th International Conference on Computing, Power and Communication Technologies (GUCON), Kuala Lumpur, Malaysia, 24–26 September 2021. [CrossRef]
175. Wilson, R.; Gandhi, R.; Kumar, A.; Roy, R. Performance Analysis of Twin-Rotor Axial Flux Permanent Magnet Synchronous Motor for In-Wheel Electric Vehicle Applications with Sensorless Optimized Vector Control Strategy. In Proceedings of the 2020 IEEE International Conference on Power Electronics, Drives and Energy Systems (PEDES), Jaipur, India, 16–19 December 2020. [CrossRef]
176. Zhao, J.; Quan, X.; Jing, M.; Lin, M.; Li, N. Design, Analysis and Model Predictive Control of an Axial Field Switched-Flux Permanent Magnet Machine for Electric Vehicle/Hybrid Electric Vehicle Applications. *Energies* **2018**, *11*, 1859. [CrossRef]
177. Akhil, R.; Mini, V.; Mayadevi, N.; Harikumar, R. Modified Flux-Weakening Control for Electric Vehicle with PMSM Drive. *IFAC-PapersOnLine* **2020**, *53*, 325–331. [CrossRef]
178. Luo, X.; Niu, S.; Fu, W. Design and Sensorless Control of a Novel Axial-Flux Permanent Magnet Machine for In-Wheel Applications. *IEEE Trans. Appl. Supercond.* **2016**, *26*, 1–5. [CrossRef]
179. Yuan, X.; Zhang, W.; Liang, X.; Hao, L.; Liang, Y. Research of Control Methods for Axial Field Flux-Switching Permanent Magnet Machine. In Proceedings of the 2018 21st International Conference on Electrical Machines and Systems (ICEMS), Jeju, Republic of Korea, 7–10 October 2018. [CrossRef]
180. Liu, C.-T.; Chiang, T.-S.; Zamora, J.D.; Lin, S.-C. Field-Oriented Control Evaluations of a Single-Sided Permanent Magnet Axial-Flux Motor for an Electric Vehicle. *IEEE Trans. Magn.* **2003**, *39*, 3280–3282. [CrossRef]
181. Mino-Aguilar, G.; Dominguez, A.M.; Maya, R.; Alvarez, R.; Cortez, L.; Munoz, G.; Guerrero, F.; Maya, S.; Rodriguez, A.M.; Portillo, F. A Direct Torque Control for a PMSM. In Proceedings of the 2010 20th International Conference on Electronics Communications and Computers (CONIELECOMP), Cholula, Mexico, 22–24 February 2010.
182. Zhong, L.; Rahman, M.F.; Hu, W.; Lim, K.; Rahman, M. A Direct Torque Controller for Permanent Magnet Synchronous Motor Drives. *IEEE Trans. Energy Convers.* **1999**, *14*, 637–642. [CrossRef]
183. Malyshev, A.; Ivanov, A. Direct Torque Control of the Axial Flux Permanent Magnet Motor. In Proceedings of the 2019 Dynamics of Systems, Mechanisms and Machines (Dynamics), Omsk, Russia, 5–7 November 2019. [CrossRef]
184. Fard, J.R.; Ardebili, M. Design and Control of a Novel Yokeless Axial Flux-Switching Permanent-Magnet Motor. *IEEE Trans. Energy Convers.* **2018**, *34*, 631–642. [CrossRef]
185. Anisi, H.; Khaburi, D.A.; Eshraghi, H.; Heshmatian, S. Elimination of Position Sensor in Direct Torque Control of Brushless Trapezoidal Axial Flux Synchronous Motor. In Proceedings of the 2017 8th Power Electronics, Drive Systems & Technologies Conference (PEDSTC), Mashhad, Iran, 16 February 2017. [CrossRef]
186. Zhao, J.F.; Hua, M.Q.; Liu, T.Z. Research on a Sliding Mode Vector Control System Based on Collaborative Optimization of an Axial Flux Permanent Magnet Synchronous Motor for an Electric Vehicle. *Energies* **2018**, *11*, 3116. [CrossRef]
187. Yang, Z.; Zhang, W.; Liang, X.; Wang, J.; Zhai, L.; Zhu, Y. Position Sensorless Control of Hybrid Excitation Axial Field Flux-Switching Permanent Magnet Machine Based on Model Reference Adaptive System. In Proceedings of the 2019 22nd International Conference on Electrical Machines and Systems (ICEMS), Harbin, China, 11–14 August 2019. [CrossRef]

188. Gurusamy, V.; Baruti, K.H.; Zafarani, M.; Lee, W.; Akin, B. Effect of Magnets Asymmetry on Stray Magnetic Flux Based Bearing Damage Detection in PMSM. *IEEE Access* **2021**, *9*, 68849–68860. [CrossRef]
189. Kolano, K. New Method of Vector Control in PMSM Motors. *IEEE Access* **2023**, *11*, 43882–43890. [CrossRef]
190. Zhai, L.; Yang, Z.; Zhang, W.; Wang, J.; Liang, X.; Zhu, Y. Speed Sensorless Control of Axial Field Flux-Switching Permanent Magnet Machine Based on Improved Adaptive Sliding Mode Observer. In Proceedings of the 2019 22nd International Conference on Electrical Machines and Systems (ICEMS), Harbin, China, 11–14 August 2019. [CrossRef]
191. Farhan, N.S.; Humod, A.T.; Hasan, F. Field Oriented Control of AFPMSM for Electrical Vehicle Using Adaptive Neuro-Fuzzy Inference System (ANFIS). *Eng. Technol. J.* **2021**, *39*, 1571–1582. [CrossRef]
192. Verkroost, L.; Druant, J.; Vansompel, H.; De Belie, F.; Sergeant, P. Performance Degradation of Surface PMSMs with Demagnetization Defect under Predictive Current Control. *Energies* **2019**, *12*, 782. [CrossRef]
193. Zhang, Y.P.; Wang, Y.M.; Gao, S.N. 3-D magnetic equivalent circuit model for a coreless axial flux permanent-magnet synchronous generator. *IET Electr. Power Appl.* **2021**, *15*, 1261–1273. [CrossRef]
194. Yang, G.; Lin, M.; Li, N.; Fu, X.; Liu, K. Maximum Torque Output Control of Hybrid Permanent Magnet Axial Field Flux-Switching Memory Machine. In Proceedings of the 2017 IEEE Energy Conversion Congress and Exposition (ECCE), Cincinnati, OH, USA, 1–5 October 2017. [CrossRef]
195. Zhang, W.; Yang, Z.X.; Zhai, L.G.; Wang, J.L. Speed Sensorless Control of Hybrid Excitation Axial Field Flux-Switching Permanent-Magnet Machine Based on Model Reference Adaptive System. *IEEE Access* **2020**, *8*, 22013–22024. [CrossRef]

https://doi.org/10.3390/app16146854